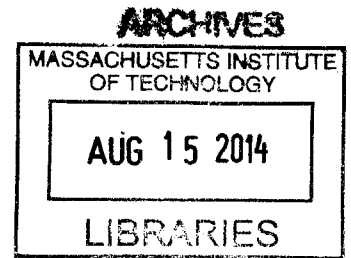


**The Effect of Lubricant Derived Ash on the Catalytic Activity of
Diesel Particulate Filters**

by

Timothy Quinn Murray

B.S., Mechanical Engineering
McGill University, 2012



Submitted to the Department of Mechanical Engineering in Partial Fulfillment of
the Requirements for the Degree of

MASTER OF SCIENCE IN MECHANICAL ENGINEERING

AT THE

MASSACHUSETTS INSTITUTE OF TECHNOLOGY

June 2014

© 2014 Massachusetts Institute of Technology
All rights reserved.

Signature redacted.

Signature of Author: _____

Department of Mechanical Engineering
May 9, 2014

Signature redacted

Certified by: _____

Principal Research Scientist and Lecturer in Mechanical Engineering
Thesis Supervisor
Victor W. Wong

Signature redacted

Accepted by: _____

David Hardt
Chairman, Department Committee on Graduate Students

(This page intentionally left blank)

The Effect of Lubricant Derived Ash on the Catalytic Activity of Diesel Particulate Filters

by

Timothy Quinn Murray

Submitted to the Department of Mechanical Engineering on May 9, 2014 in Partial Fulfillment of the Requirements for the Degree of

MASTER OF SCIENCE IN MECHANICAL ENGINEERING

ABSTRACT

A diesel particulate filter (DPF) is an aftertreatment device used to remove hazardous particulate matter (PM) from diesel engine exhaust. Modern emission restrictions have limited the acceptable amount of PM output by diesel engines to the extent that a filtration strategy, such as the use of a DPF, is necessary.

Diesel PM is comprised primarily by black carbon soot. Once trapped in the filter, the soot can be oxidized into CO₂ and pass out of the exhaust system during what is referred to as regeneration. Metallic lubricant additive derived compounds, which make up a small fraction of PM, cannot be oxidized and remain inside the DPF until regular maintenance calls for the removal and cleaning of the filter. The buildup of ash increases the pressure drop across the filter, resulting in a direct fuel penalty to the engine.

The oxidation of soot can be carried out actively at high temperatures or passively at low temperatures with the aid of a catalyst. Active regeneration requires more energy than passive regeneration because the stream of exhaust gas must be heated to a higher temperature. However, catalysts are expensive, and therefore there is a significant additional capital cost associated with catalyzed filters.

The purpose of this research was to investigate the impact of ash accumulation on the catalytic activity of DPFs. The impact was measured experimentally by comparing the ability of two ash loaded DPF samples to promote several chemical reactions (most importantly soot oxidation) to the ability of a previously unused (clean) filter.

It was shown that ash accumulation results in a loss in the catalytic activity of a DPF, as evidenced by a reduced capacity to generate NO₂, and promote the catalyzed passive oxidation of soot. Reduced soot oxidation performance will result in faster accumulation of soot, which increases the pressure drop across the filter and necessitates more frequent regenerations. Both of these results will negatively impact fuel economy.

Thesis Supervisor: Victor W. Wong

Title: Principal Research Scientist and Lecturer in Mechanical Engineering

(This page intentionally left blank)

ACKNOWLEDGMENTS

My time at MIT has been a challenging and rewarding experience that I will carry with me always. Countless people have helped me along the way, and to all of them I owe a great deal of thanks. I would like to take this opportunity to single out a special few.

My advisor, Dr. Victor Wong, has been a constant source of guidance throughout my degree. I would like to thank him for the opportunity to work on this project, which I believe was both interesting and important. I would also like to thank Dr. Carl Justin Kamp and Dr. Alex Sappok for their direction and advice. Both of them were not only vital technical resources, but also taught me how scientific research should be conducted and strengthened my critical thinking and problem solving skills. I had the privilege of working in a wonderful group; thank you to all of my lab mates: Casey Chiou, Michael Bahr, Yujun Wang, James Jorgenson, Nicholas Custer, and Paul Folino. Additionally, Thane DeWitt and Raymond Phan provided me with a tremendous amount of help setting up and repairing all of the experimental apparatuses used in this study.

The research I have conducted would not have been possible without the support of the MIT Consortium to Optimize Lubricant and Diesel Engines for Robust Emission Aftertreatment Systems. Thank you to all current and past members of this organization both for funding my project, as well as all of the invaluable discussions during our meetings.

Finally, and most importantly, I would like to thank my family and friends. To those I've made here in Boston and to those back home, thank you. I could not have done it without you. Thank you to my Mom and Dad, my brothers Andrew and Peter, and my Baba and Grandpa. You got me here. You got me through it. I can't thank you enough.

(This page intentionally left blank)

Table of Contents

ACKNOWLEDGMENTS	5
LIST OF FIGURES	9
LIST OF TABLES	11
ABBREVIATIONS	13
1 INTRODUCTION	15
1.1 Diesel Engine Fundamentals.....	15
1.1.1 Diesel Engine Advantages.....	17
1.1.2 Diesel Engine Applications.....	18
1.1.3 Diesel Engine Emissions.....	19
1.2 Diesel Emissions Regulations	21
1.3 Emissions Reduction Methods.....	24
2 DIESEL PARTICULATE FILTERS	27
2.1 DPF Operation.....	27
2.2 Regeneration.....	28
2.3 Ash Accumulation.....	29
2.3.1 Ash Sources	30
2.3.2 Ash Transport.....	31
2.3.3 Effects of Ash on DPF Pressure Drop	32
3 DPF CATALYTIC ACTIVITY	35
3.1 CATALYST FUNDAMENTALS	35
3.2 DPF Catalysts.....	37
3.3 Catalyzed Oxidation of Soot	38
3.4 Modes of Catalyst Deactivation	39
3.4.1 Catalytic Deactivation through Physical Masking/Poisoning.....	39

3.4.2	Catalytic Deactivation through Thermal Aging.....	40
3.5	Effects of Ash Accumulation on DPF Catalysts	41
4	EXPERIMENTAL SET-UP AND TECHNIQUES	45
4.1	Accelerated Ash Loading System	45
4.2	DPF Ash Loaded Samples.....	47
4.3	DPF Core Sample Soot Loading System	50
4.4	Catalyst Flow Bench Reactor	51
4.4.1	Catalyst Flow Bench System Improvements	54
5	EXPERIMENTAL TESTING AND RESULTS	57
5.1	Gaseous Conversion in the DPF	57
5.1.1	CO + HC + NO Oxidation.....	60
5.1.2	CO and HC Conversion.....	62
5.1.3	Desorption	64
5.1.4	NO Oxidation	65
5.1.4.2	Isothermal NOx Step Experiment	72
5.2	Soot Oxidation.....	75
5.2.1	Temperature Ramp.....	75
5.2.2	Isothermal Soot Oxidation	81
6	CONCLUSIONS	85
6.1	Summation of Results	85
6.2	Suggestions for Future Research.....	87
7	REFERENCES	89
	APPENDIX.....	93

LIST OF FIGURES

Figure 1.1 Start of Combustion in Gasoline SI vs. Diesel Engine.....	16
Figure 1.2 Idealized Otto and Diesel Cycle P-v Diagrams	17
Figure 1.3 Diesel Penetration in the EU15 + EFTA (% of new registrations) 1990-2012 ⁸	19
Figure 1.4 EPA Heavy Duty Diesel Emissions Regulations	22
Figure 1.5 US EPA Tier 3 NMOG + NOx FTP Emissions Standard	23
Figure 1.6 Diesel Engine Aftertreatment System Configuration.....	25
Figure 2.1 Wall-flow and Flow-through Filter Flow Patterns	27
Figure 2.2 Depth vs. Cake Filtration Mechanisms ¹⁷	28
Figure 2.3 Percent Oxidation of Carbon vs. Time at Different Temperatures	29
Figure 2.4 Ash and Soot Buildup in a DPF	30
Figure 2.5 Schematic Representation of Ash Particle Formation and Growth over Repeated DPF Regeneration ²⁹	31
Figure 2.6 Conceptual Illustration of Ash Distribution in a DPF over Time ³¹	32
Figure 2.7 Effect of Ash on DPF Pressure Drop	33
Figure 2.8 Effect of Soot and Ash on DPF Pressure Drop ²⁹	34
Figure 3.1 Effect of Catalyst on Activation Energy	36
Figure 3.2 Pictorial Representation of Catalyst Distribution on a DPF Surface	37
Figure 3.3 Illustration of Catalyzed Oxidation of Soot.....	38
Figure 3.4 SEM Image of Soot-DPF Interface	39
Figure 3.5 Illustration of Catalytic Deactivation via Poisoning/Fouling ³⁷	40
Figure 3.6 Illustration of Catalytic Deactivation through Thermal Aging ³⁷	41
Figure 3.7 SEM Image of Ash Coating Catalyst Particles ⁴²	42
Figure 3.8 SEM Images of Stratified DPF-Ash-Soot Layers ⁴²	43
Figure 3.9 Illustration of Ash Layer Impact on Catalytic Reaction ⁴⁰	43
Figure 3.10 X-Ray CT Image of DPF Core Sample.....	43
Figure 4.1 Schematic of Accelerated Ash Loading System ²³	46
Figure 4.2 Illustration of DPF Core Sample Geometry ⁴³	49
Figure 4.3 Close-up Image Used to Measure Ash Layer Thickness ⁴³	49
Figure 4.4 Ash Layer Distribution in 42 g/L (280,000 mi) DPF Sample ⁴³	49
Figure 4.5 Canned DPF Core Samples	50

Figure 4.6 Schematic of DPF Core Sample Soot Loading Apparatus	51
Figure 4.7 Schematic of Flow Bench Reactor	52
Figure 4.8 DPF Thermal Stability during CO, HC, and NO Oxidation.....	53
Figure 4.9 Updated Catalyst Flow Bench Schematic	54
Figure 5.1 Simultaneous Conversion of CO, HC, and NO in a DPF.....	60
Figure 5.2 NO/NO ₂ Thermodynamic Equilibrium as Calculated by a Thermodynamic Model ⁴³	61
Figure 5.3 Ash Effect on CO Oxidation Light-off Temperature	62
Figure 5.4 Ash Effect on HC Oxidation Light-off Temperature	63
Figure 5.5 Gaseous Emissions from Clean and 12.5 g/L Ash Loaded DPF Desorbed from Surface during Temperature Ramp	64
Figure 5.6 NO Oxidation in Clean DPF: Flow Velocity Dependence.....	66
Figure 5.7 Ash Effect on NO Oxidation at 20,000 hr ⁻¹	67
Figure 5.8 Ash Effect on NO Oxidation at 40,000 hr ⁻¹	67
Figure 5.9 Ash Effect on NO Oxidation at 60,000 hr ⁻¹	68
Figure 5.10 Peak NO Destruction for Clean and Ash Loaded Samples at Various Flow Velocities	69
Figure 5.11 X-Ray CT Scans from 42 g/L Ash Loaded DPF Core Sample	70
Figure 5.12 X-Ray CT Scan of 12.5 g/L Ash Loaded DPF Core Sample	70
Figure 5.13 NO Oxidation at 40,000 hr ⁻¹ : Velocity Adjusted for Ash Plug Volume	71
Figure 5.14 NO Oxidation at 60,000 hr ⁻¹ : Velocity Adjusted for Ash Plug Volume	72
Figure 5.15 Clean DPF Isothermal NO Oxidation.....	73
Figure 5.16 42 g/L Ash Loaded DPF Isothermal NO Oxidation.....	73
Figure 5.17 Isothermal NO to NO ₂ Conversion with increasing NO Concentration.....	74
Figure 5.18 Direct Measurement of CO ₂ output from Clean DPF during Regeneration.....	76
Figure 5.19 Plot of Formation Rate vs. Temperature for a Clean DPF during Regeneration	78
Figure 5.20 Arrhenius Plot: Soot Oxidation Reaction for Clean DPF.....	79
Figure 5.21 Arrhenius Plot of Soot Oxidation Reaction: Active Oxygen Mechanism (>525°C) for Clean and 42 g/L Ash Loaded DPFs.....	80
Figure 5.22 Arrhenius Plot of Soot Oxidation Reaction: Passive NO ₂ Mechanism (325-425°C) for Clean and 42 g/L Ash Loaded DPF	80

Figure 5.23 Isothermal Soot Oxidation Reaction of Clean and 42 g/L Ash Loaded DPFs (10 minutes)..... 82

Figure 5.24 Isothermal Soot Oxidation Reaction of Clean and 42 g/L Ash Loaded DPFs (1 hour) 83

LIST OF TABLES

Table 1-1 US EPA Tier 3 PM FTP Emissions Standard¹⁶ 23

Table 4-1 Accelerated Ash Loading System Parameter Specifications⁴³ 46

Table 4-2 Elemental Analysis of the Test Fuel⁴³ 47

Table 4-3 Elemental Analysis of Test Oil⁴³ 48

Table 4-4 Laboratory-Aged DPF Sample List..... 48

Table 4-5 Pramac S5500 Yanmar L100V Generator Specifications 50

Table 5-1 Typical Concentrations of Diesel Engine Emissions⁴⁸ 58

Table 5-2 DPF Gaseous Conversion Test Matrix 59

(This page intentionally left blank)

ABBREVIATIONS

Al ₂ O ₃	Alumina (Aluminum Oxide)
ATS	Aftertreatment System
C ₃ H ₆	Propylene (Propene)
Ca	Calcium
CARB	California Air Research Board
CI	Compression ignition
CO	Carbon monoxide
CO ₂	Carbon dioxide
COPD	Chronic Obstructive Pulmonary Disease
CT	Computed Tomography
DOC	Diesel Oxidation Catalyst
DPF	Diesel Particulate Filter
DRIFTS	Diffuse Reflectance Infrared Fourier Transform Spectroscopy
EGR	Exhaust Gas Recirculation
EPA	Environmental Protection Agency
FIB	Focused Ion Beam
FTIR	Fourier Transform Infrared Spectroscopy
HC	Hydrocarbon
IC	Internal combustion
Mg	Magnesium
MIT	Massachusetts Institute of Technology
N ₂	Nitrogen
NO	Nitrogen monoxide/nitric oxide
NO ₂	Nitrogen dioxide
NO _x	Nitrogen oxides
O ₂	Oxygen
PGM	Platinum Group Metal
PM	Particulate matter
Pt	Platinum
SCR	Selective Catalytic Reduction
SEM	Scanning Electron Microscopy
SI	Spark ignition
SO ₂	Sulfur Dioxide
SOF	Soluble Organic Fraction
TDC	Top dead center
TWC	Three Way Catalyst
ULSD	Ultra Low Sulfur Diesel
Zn	Zinc

$\eta_{f,i}$	Indicated Fuel Conversion Efficiency
c_p	Specific Heat Capacity at Constant Pressure
c_v	Specific Heat capacity at Constant Volume
r_c	Compression Ratio
γ	Heat Capacity Ratio
E_a	Activation Energy
ΔP	Pressure Drop (Backpressure)
μ	Gas Dynamic Viscosity
k	Permeability
A	Filter Surface Area
Q, \dot{V}	Volumetric Flow Rate
n_x	Moles of Species 'x'
V	Volume
P	Pressure
\bar{R}	Universal Gas Constant
T	Temperature
MW_C	Molecular Weight of Carbon
X_c	Fraction of Unburnt Carbon
$m_{c,i}$	Initial Mass of Carbon
t	Arbitrary Time Step
t_i	Initial Time (Onset of Experiment)
t_f	Final Time (End of Experiment)

1 INTRODUCTION

The transportation sector comprises roughly 20% of global energy consumption; within the United States of America the figure rises to 28%.¹ As the cost of energy continues to increase and the impact of energy usage continues to alter the world's environment it is important to improve the means of reducing the consumption of energy by all available options. The diesel engine is the most energy efficient powerplant among currently available internal combustion (IC) engines, which makes it an attractive option for the transportation sector. In 2012 diesel fuel accounted for 21% of the total fuel used for transportation in the United States of America.¹ It is the primary fuel in almost all commercial freight operations, and has become a significant portion of the passenger vehicle fleet, particularly in markets, like Europe, which have exceptionally high fuel prices. One major obstacle facing diesel engines is their propensity to output particulate matter (PM) which has been linked to several adverse health effects. Concern for public health has prompted strict emissions regulations limiting the acceptable level of PM output by an engine.

While the operation of a diesel engine can be manipulated to reduce the PM generated, a reduction to zero or near-zero level has not been possible through engine operation strategy alone. Therefore, an aftertreatment device must be employed to remove the particulates from the exhaust stream. The diesel particulate filter (DPF) has emerged as the preeminent filtration technology. DPFs have been employed on virtually every diesel powered engine produced in the United States or Europe since 2007, and have been found to reduce engine-out soot emissions by more than 90%.² While the existing DPF technology has proven very useful in reducing the output of particulate matter from diesel engines, it has numerous complex effects on engine performance, which has motivated extensive research into the design, operation and durability of the device. This study focuses on the effect of ash on the catalytic activity of diesel particulate filters and the resulting implications for carbonaceous soot oxidation.

1.1 Diesel Engine Fundamentals

The diesel engine was originally conceived and constructed by Rudolf Diesel at the end of the nineteenth century. Since that time there have been significant improvements to its design but the underlying mechanism remains the same. Similar to a standard gasoline engine, the diesel engine

uses a reciprocating piston within a cylinder coupled to a slider crank mechanism to rotate a shaft. The fundamental difference between a diesel combustion ignition (CI) and a conventional spark ignition (SI) engine is the source of ignition. A diesel relies on the high temperature and pressure of the intake air near the top dead center (TDC) of the compression stroke to auto-ignite the fuel which is injected either directly into the combustion chamber or an adjacent pre-combustion chamber. A gasoline SI engine, on the other hand, initiates combustion with an electrical spark within the air-fuel mixture.

In a gasoline SI engine the flame front will expand quasi-spherically outwards from the spark, combusting the air-fuel mixture which is maintained as nearly stoichiometric. In contrast, the diesel fuel is injected directly into the combustion chamber where it spontaneously combusts due to the high pressure and temperature. Although the overall mixture is lean in a diesel engine, the fuel is atomized during injection into small droplets which locally burn rich as a diffusion flame. As a result soot is formed in the wake of the injected fuel in particularly high concentrations along the spray axis near the injector nozzle.³

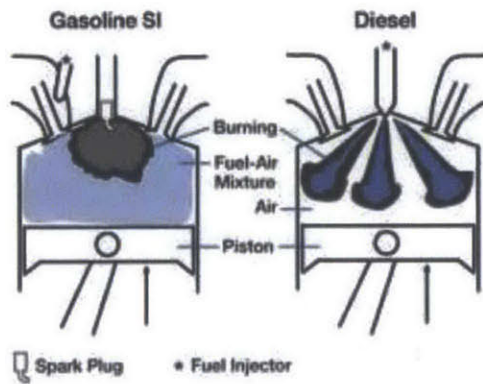


Figure 1-1 Start of Combustion in Gasoline SI vs. Diesel Engine⁴

Another major difference between gasoline and diesel engines is the way in which each engine meters its power. An SI engine limits the engine load by throttling the air entering the combustion chamber, whereas a diesel engine restricts the amount of fuel injected. Since there is no fuel in the diesel engine cylinder during compression, there is no risk of inducing early combustion, otherwise known as knock, which is a major limiting factor in the compression ratios of SI engines. As a result, diesel engines are able to operate at compression ratios that are significantly higher than gasoline engines.

1.1.1 Diesel Engine Advantages

The primary advantage of the diesel engine as compared to other IC engines is its superior energy efficiency. The operation of both CI and SI engines can be idealized by the Diesel and Otto cycles respectively as depicted by Figure 1-2. It is assumed that the working fluid is an ideal gas with constant c_v and c_p and that each portion of the cycle occurs at constant pressure, volume, or entropy (isentropic) as shown in Figure 1-2.

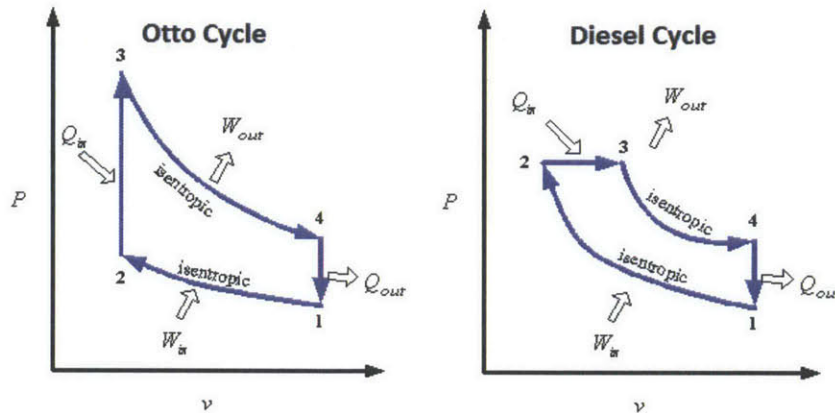


Figure 1-2 Idealized Otto and Diesel Cycle P-v Diagrams⁵

Under these idealized conditions the indicated fuel conversion efficiencies of each cycle can be determined, as described by Eq. 1-1 and Eq. 1-2.

Eq. 1-1

$$\eta_{f,i \text{ otto}} = 1 - \frac{1}{r_c^{\gamma-1}}$$

Eq. 1-2

$$\eta_{f,i \text{ diesel}} = \left(1 - \frac{1}{r_c^{\gamma-1}}\right) \left[\frac{\beta^\gamma - 1}{\gamma(\beta - 1)}\right]$$

Where:

$$r_c = \frac{v_2}{v_1} = \text{compression ratio}$$

$$\gamma = \frac{c_p}{c_v}$$

$$\beta = \frac{v_3}{v_2}$$

For a given compression ratio the SI engine will have the higher efficiency; however, as described in *Section 1.1*, a diesel engine is able to operate with a higher compression ratio because there is much less risk of knock, and it is therefore able to reach a greater overall efficiency. A typical value for r_c of a spark ignition engine is 8-12, while a compression ignition engine can reach values from 12-24.³ Additionally, since a diesel engine always operates lean the value of γ is higher than that of an SI engine.³

The heat from combustion is released both earlier and faster in a diesel engine compared to a typical gasoline engine. This has two direct results: first, it generates higher torque at lower speeds, i.e., higher power at low speeds. Since friction is proportional to engine speed there is typically less frictional loss for a diesel engine operating at the same load as a SI engine; second, it demands more robust manufacturing standards, which contribute to higher costs but also greater durability. Often diesel engines are able to operate for over 1 million miles before requiring a total overhaul.⁶

Diesel engines control their power output by varying the amount of fuel injected into the cylinder as opposed to throttling the incoming air. As a result there is significantly lower pumping loss, which translates to improved efficiency and fuel economy. Overall, diesel engines have been found to exhibit an improvement in fuel economy of 30-35% compared to similar-sized gasoline engines.⁷

Another advantage of diesel engines is that they produce significantly less pollution as compared to a standard SI engine. Since the combustion mixture is lean, there is ample oxygen available to combust all of the hydrocarbons (HC) and convert any carbon monoxide (CO) to carbon dioxide (CO₂). As a result the concentration of hydrocarbons in diesel exhaust is lower than that of a standard SI engine by a factor of 5, and the amount of CO emitted is practically negligible.³

1.1.2 Diesel Engine Applications

As a result of its high fuel efficiency and durability the diesel engine has become the powerplant of choice for a wide range of applications. It dominates the transportation of freight by trucks, trains, and boats, accounting for 94% of all goods shipped in the USA.¹ It is also used in over two-thirds of all agricultural equipment in the USA,¹ and has been widely used in buses, construction equipment and electrical generators to name only a few of its many applications.

While diesel powered personal vehicles have not been widely adopted by American consumers, they constitute a significant and growing portion of the European market. In 2012, 35.9% of all passenger vehicles in use were powered by diesel engines, up 0.6% from 2010⁸. Figure 1-3 clearly shows the upward trend in diesel car ownership as indicated by the increasing percentage of new vehicle registrations, which has increased from roughly 12% to greater than 50% in the last 20 years.

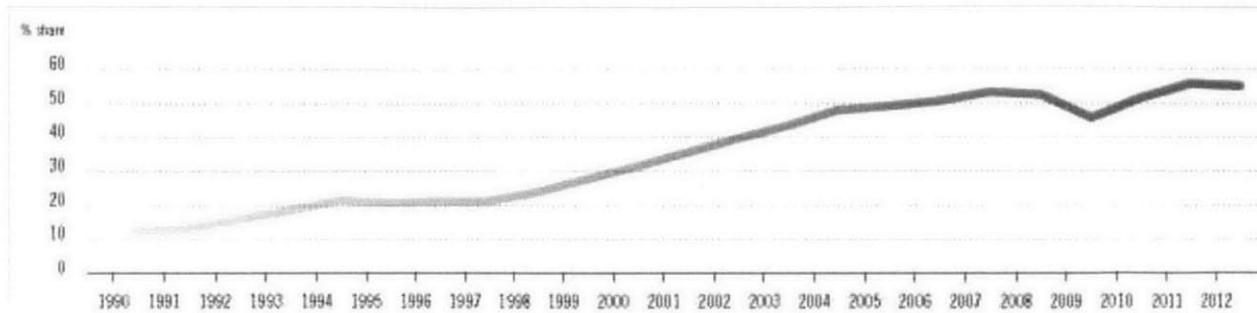
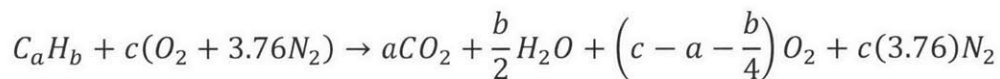


Figure 1-3 Diesel Penetration in the EU15 + EFTA (% of new registrations) 1990-2012⁸

1.1.3 Diesel Engine Emissions

The fundamental purpose of an IC engine is to convert the chemical energy stored in fuel to useful mechanical work. This purpose is achieved by harvesting the energy released during a combustion reaction between hydrocarbons and oxygen present in the air. The simplest form of this combustion reaction is shown in Eq. 1-3.

Eq. 1-3



Since the fuel is injected into the air directly before combustion there is little time for mixing, and a homogeneous charge is virtually impossible. As a result, as more fuel is added to the mixture, i.e., approaching stoichiometric conditions, it becomes difficult to utilize all of the available oxygen resulting in incomplete combustion and the production of excessive amounts of soot. To combat this, the mixture is always operated lean so that there is ample oxygen available to combust all of the fuel. Thus in Eq. 1-3 $c > a + \frac{b}{4}$. At full load diesel engines generally maintain a fuel/air ratio greater than 20% above stoichiometric.³

Eq. 1-3 is in fact an idealized reaction; in reality, several factors contribute to imperfect combustion, each of which results in undesirable emissions, primarily in the form of unburnt

hydrocarbons (HC), nitrogen oxides (NO_x), and particulate matter (PM). Carbon monoxide (CO) is also produced, but as noted in *Section 1.1.1*, the concentrations are very low.

Hydrocarbons found in diesel exhaust are the result of unburnt or partially decomposed fuel and, to a lesser extent, burnt lubricating oil that has formed a film layer on the cylinder walls.⁹ As described in *Section 1.1.1*, HC emissions are generally significantly lower than those of an SI engine. In a CI engine the overall mixture is lean, so there should be sufficient oxygen to fully react the fuel. An SI engine, which oscillates between rich and lean on a cycle to cycle basis, will produce more HC during individual rich combustion events. Additionally, since there is no fuel in the cylinder of a CI engine before injection, fuel does not get trapped in the crevice volumes within the cylinder to be released during the expansion and exhaust stroke; whereas, in an SI engine, fuel trapping does occur and is a major source of HC emissions.

NO_x refers to oxides of nitrogen primarily in the form of nitrogen monoxide, i.e., nitric oxide (NO), which accounts for 70-90% of the total NO_x in diesel exhaust, and nitrogen dioxide (NO₂), which makes up the bulk of the remaining NO_x.⁹ NO forms within the high temperature burned gas, preferentially in regions where the heterogeneous mixture is near stoichiometric.³ The amount of NO_x produced by a diesel CI engine is comparable to that of a gasoline SI engine;³ however, since the exhaust from a diesel engine is lean the NO_x cannot be converted to nitrogen and oxygen via a three way catalyst (TWC) or catalytic converter as on a typical gasoline engine.

Particulate matter comprises all solid materials entrained in the flowing exhaust gas. It primarily consists of agglomerates made up of solid carbon and lubricant derived ash (approximately 54% by mass), soluble organic fraction (SOF) (approximately 32% by mass), and sulfates (approximately 14% by mass).¹⁰ Additionally, trace amounts of iron particles resulting from engine wear and even dust or debris from the intake air can be found as PM in the exhaust. Soot, which makes up the vast majority of solid particles that are trapped in diesel particulate filters, is formed in fuel-rich regions of the unburned flame, particularly at the centerline of the injection spray.

Due to the complex nature in which these emissions form, it is difficult to reduce their presence through a single strategy. It is particularly difficult to simultaneously reduce NO_x and PM

emissions; this challenge is typically referred to as the *NOx-PM trade-off*. Many strategies used to reduce NOx emissions, such as retarded ignition timing or reduced combustion temperatures through exhaust gas recirculation (EGR), result in increased PM emissions.¹¹ Similarly, many techniques used to decrease PM will result in increased NOx. Of course, these emissions reduction strategies are also coupled to engine performance, which increases the complexity of the problem.

1.2 Diesel Emissions Regulations

Diesel emissions have a significant adverse effect on human health. Diesel particulate matter is a known carcinogen; it has been linked to numerous respiratory health issues including asthma, lung cancer, and chronic obstructive pulmonary disease (COPD).¹² NO₂ is a powerful toxin that causes a pulmonary edema – the buildup of fluid in the air sacs of the lungs – in concentrations as low as 5 ppm.¹³ Nitric oxide (NO) on its own acts as an irritant to the eyes and lungs, but is even more dangerous due to its instability in air which causes it to spontaneously react to form highly toxic NO₂. Research reports indicate that 80 ppm NO would form 5 ppm of NO₂ in only 3 minutes.¹³

In addition to their direct effect on humans, diesel emissions alter the natural environment. NOx reacts with volatile organic compounds to form ground level ozone, otherwise known as smog, and particulate matter contributes to haze in the air and increases the acidity of lakes, streams, and soil in which it settles.¹⁴ Soot will also exhibit a significant greenhouse effect due to its ability to re-radiate heat.

Concern over the adverse health and environmental effects of diesel engine exhaust has resulted in strict emissions regulations that have been consistently tightened since 1990. These regulations are controlled nationally in the United States by the Environmental Protection Agency (EPA), as well as by each individual state, which is free to implement stricter policies than those enacted on the national level. The state of California has been particularly active in passing legislation tightening emissions restrictions, which are managed by the California Air Research Board (CARB).

The EPA regulations are divided into different categories representing different applications: heavy duty trucks and buses, cars and light duty trucks, non-road engines, locomotives, etc. Each

of these sectors has seen the acceptable levels of PM, HC, NO_x, and CO drop gradually over time allowing for technological innovation to achieve the necessary standards. The acceptable level of sulfur in diesel fuel has also been dramatically reduced to ensure the sulfur does not poison the catalysts in aftertreatment systems (ATS). Between 2006 and 2010 ultra-low sulfur diesel (ULSD), which limits the acceptable level of sulfur content in fuel to 15 ppm, was adopted as the standard fuel grade for all diesel in the USA.

Currently all engines in the USA must adhere to the EPA's Tier 2 standard that was phased in between 2004-2009. The heavy duty diesel emissions regulations over this period and before have been summarized below in Figure 1-4. The acceptable levels of both particulates by mass and noxious emissions have been reduced by more than an order of magnitude over that period.

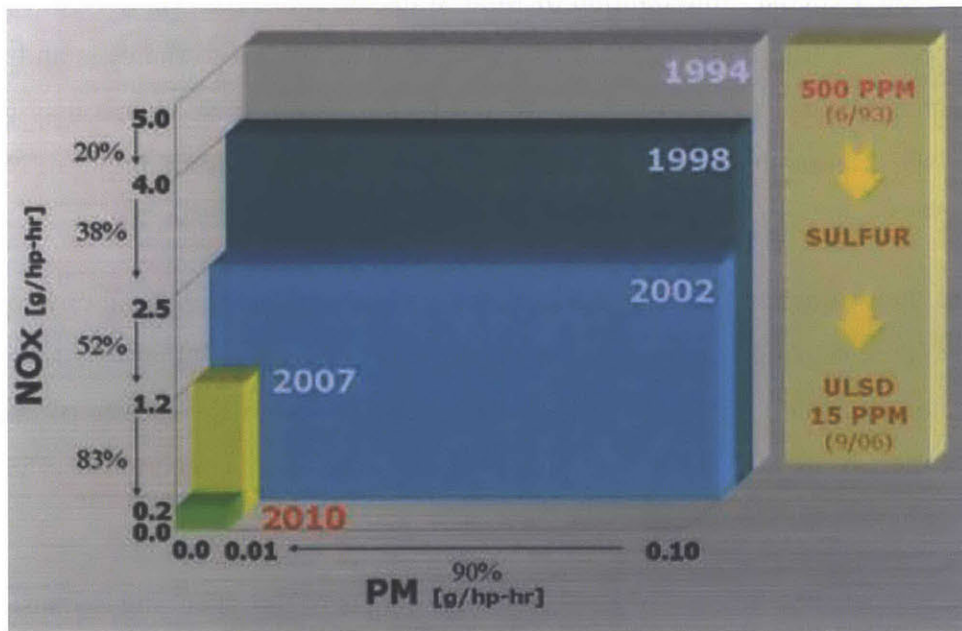


Figure 1-4 EPA Heavy Duty Diesel Emissions Regulations¹⁵

On March 3, 2014 the next stage of emission standards, Tier 3, was signed into law, and is scheduled to be phased in from 2017-2025. It will further reduce acceptable levels of NO_x, PM, and HC to levels similar to those imposed by the CARB. The combined non-methane organics (NMOG) and NO_x emissions limits are displayed in Figure 1-5.

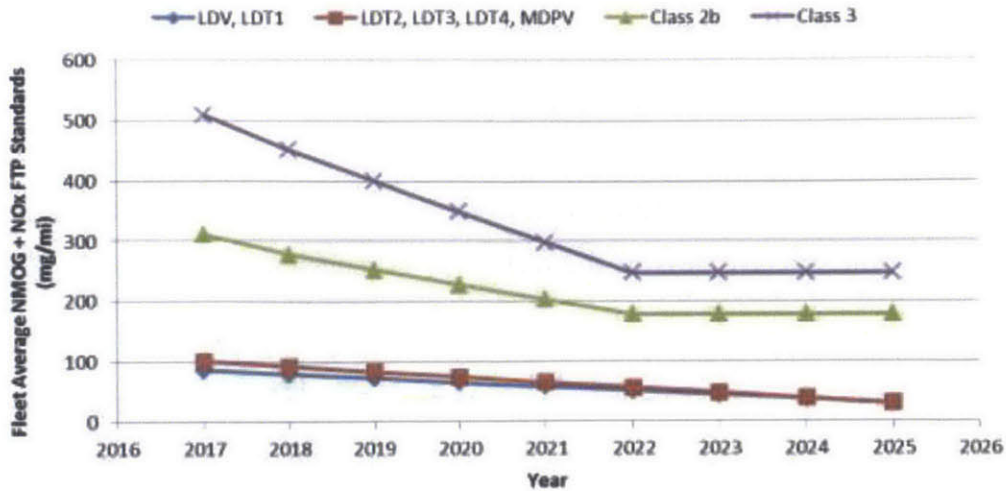


Figure 1-5 US EPA Tier 3 NMOG + NOx FTP Emissions Standard¹⁶

Under the Tier 3 standard, PM is to be limited to 3 mg/mi per vehicle over the FTP -75 testing standard. Unlike NOx emissions, in which a fleet average is computed for each manufacturer, each vehicle must be certified to meet this standard individually. In order to allow for the phase-in period for new technology the percentage of new vehicles sold that must adhere to this standard will be increased from a modest 20% in 2017 to full compliance in 2021. During this phase-in period a less rigorous standard of 6 mg/mi will be considered acceptable, but re-certification would be required by 2022. Full details of the adoption schedule are outlined in Table 1-1.

Table 1-1 US EPA Tier 3 PM FTP Emissions Standard¹⁶

	Year	2017	2018	2019	2020	2021	2022
% of Sales	%	20	20	40	70	100	100
Certification Standard	mg/mi	3	3	3	3	3	3
In-use Standard	mg/mi	6	6	6	6	6	3

Hydrocarbon and carbon monoxide emissions are also regulated for diesel engines in the same way as they are for SI engines, but since their output is significantly lower there is no difficulty in meeting these standards.

1.3 Emissions Reduction Methods

There are two effective ways to reduce engine emissions: (1) improved design of the engine to reduce in-cylinder production of emissions, and (2) utilization of aftertreatment devices designed to clean up the exhaust before being emitted to the atmosphere. In either case, it is essential to consider not only the effectiveness of the technique in reducing emissions, but also its overall impact on engine performance.

A number of techniques have been employed to reduce in-cylinder production of emissions. For example, engine geometry in the intake port and cylinder has been optimized to increase the degree of turbulence in the intake air and thereby improve the mixing/dispersal of the fuel; these measures result in a reduction of the amount of PM generated. As mentioned in *Section 1.1.3*, delayed ignition timing and EGR can be used to lower combustion temperatures, reducing the NO_x generated during combustion.

Despite major improvements in diesel engine design, it has thus far not been possible to reach modern emissions expectations through this strategy alone, and therefore it has been necessary to develop aftertreatment systems. The purpose of these systems is similar to that of a catalytic converter on an SI engine, but the excess oxygen resulting from lean combustion in a diesel engine makes the operation of the gasoline three way catalyst (TWC) impossible.

A standard diesel aftertreatment system is divided into three separate devices, each designed to accomplish one task. The typical arrangement of these components is depicted in Figure 1-6. First, the exhaust gas passes through a diesel oxidation catalyst (DOC), a flow-through filter that utilizes platinum group metal (PGM) catalysts to oxidize any remaining hydrocarbons, carbon monoxide, and much of the SOF on the PM while also converting a significant portion of the NO to NO₂. Next, the flow enters the diesel particulate filter (DPF), the primary function of which is to remove all particulate matter from the exhaust. DPFs will be discussed extensively in *Section 2*. Finally, the exhaust passes through a NO_x conversion device, the most common of which is selective catalytic reduction (SCR). SCR utilizes a vanadia and zeolite based catalyst to convert NO_x to nitrogen and water through a reaction with ammonia that is introduced upstream of the device in the form of urea.

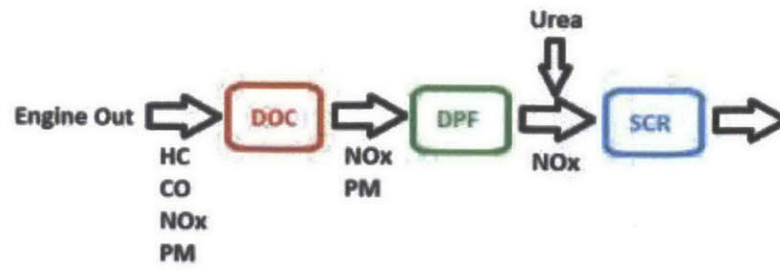


Figure 1-6 Diesel Engine Aftertreatment System Configuration

(This page intentionally left blank)

2 DIESEL PARTICULATE FILTERS

Diesel particulate filters (DPF) have emerged as the preferred aftertreatment device used to remove solid particulate matter from CI engine exhaust. First introduced in 1985 in the Mercedes-Benz 300D 3.0 turbodiesel sold in California, the device was not widely used until the early 2000s. They are now found on every diesel engine produced in the USA since 2007. The success of the DPF is primarily due to its excellent ability to filter solid particulates, reducing engine out soot by over 90%, as well as its excellent thermal and mechanical durability.²

2.1 DPF Operation

Several DPF designs have been explored since its initial introduction, but the ceramic wall-flow monolith is by far the most widely used technology today. This style of filter consists of a honeycomb structure of small channels that are parallel in the axial direction and alternatively capped on each end to produce a checkerboard pattern. As shown in Figure 2-1, the caps on the wall-flow filter force the flow to pass through the porous walls; this is unlike that of the flow-through filter in which the flow passes straight through. The filter itself typically consists of a cordierite or silicon carbide substrate that is coated with an inert base-metal washcoat layer and which may or may not be loaded with PGM catalyst particles. The pores of the substrate are large enough to allow the exhaust gas to flow through with minimal pressure drop, while they are small enough to physically block and trap particulate matter.

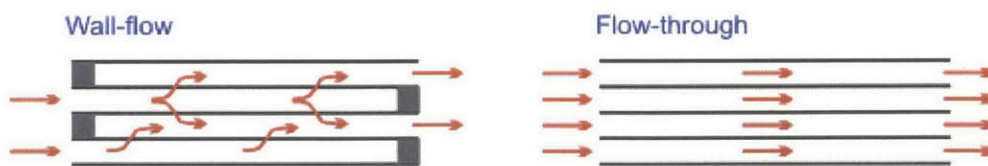


Figure 2-1 Wall-flow and Flow-through Filter Flow Patterns¹⁷

Particulate matter deposits on the wall of the filter via two distinct mechanisms: deep-bed (i.e., depth filtration) and cake filtration. During soot loading the filter will first experience deep bed penetration as PM is deposited inside the surface pores of the filter. Once a sufficient amount of soot builds up, the PM will begin to form a cake layer above the filter surface. This soot layer remains permeable to the flow of exhaust gas as the cake itself is also porous. Deep-bed filtration

is particularly costly to the filter in terms of pressure drop since it is filling and covering pores which reduces or restricts the possible pathways for exhaust flow.

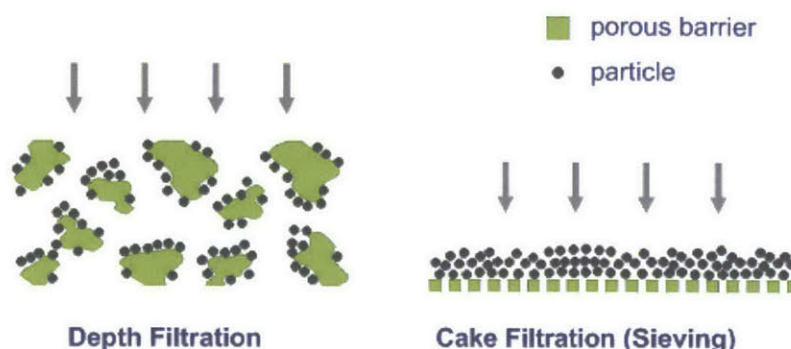


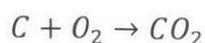
Figure 2-2 Depth vs. Cake Filtration Mechanisms¹⁷

As the PM builds up in the filter it further obstructs the flow of exhaust, increasing the pressure drop across the filter, and reducing the fuel economy of the engine. The soot can be removed from the filter through oxidation – otherwise known as “regeneration.” This can be done either actively by oxidizing the soot at high temperatures using oxygen or passively through catalyzed oxidation of the soot using NO_2 .

2.2 Regeneration

Active soot regeneration, as described by Eq. 2-1, is primarily used in a periodic cycle. Once a certain level of soot loading is reached, regeneration is induced by spiking the temperature of the exhaust gas. Figure 2-3 illustrates the strong dependence of active regeneration on temperature. Light-duty diesel engine exhaust is typically as low as 100-250°C,^{18,19} but in order to ensure timely and complete oxidation it is necessary to achieve temperatures as high as 600°C. This can be achieved in a number of ways, the most common of which is to inject extra fuel either directly into the cylinder post-injection or into the exhaust. In either case the excess HC is exothermically oxidized in the DOC upstream of the DPF, causing an increase in the exhaust temperature.²⁰ Though effective, active regeneration requires a significant amount of energy to increase filter temperature to the required level, and that results in a direct fuel penalty.

Eq. 2-1



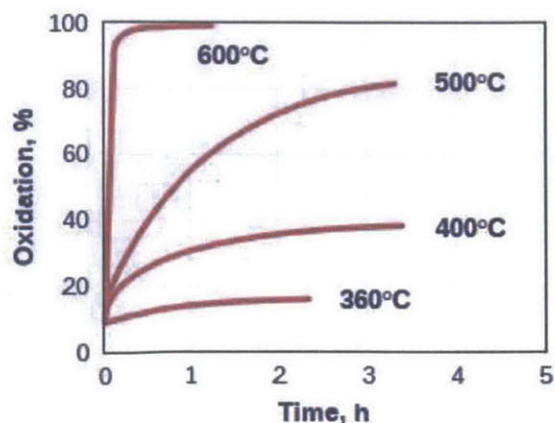
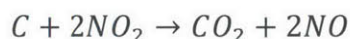


Figure 2-3 Percent Oxidation of Carbon vs. Time at Different Temperatures²¹

Passive regeneration, as described by Eq. 2-2, is achieved at much lower temperatures through the use of NO_2 instead of O_2 to oxidize the PM. It has been found that soot can be converted to CO_2 at temperatures as low as 250°C using the NO_2 mechanism. If the exhaust temperatures through the DPF are sufficiently hot enough during regular operation the soot may be oxidized continuously without the need to periodically spike the temperature. If not, additional fuel must be consumed to increase the temperature, but the penalty will be much lower than that of active regeneration since it requires significantly less energy. The major drawback of passive regeneration is the additional up-front cost associated with adding a catalyst.

Eq. 2-2



2.3 Ash Accumulation

In addition to the carbonaceous soot, PM also contains incombustible ash compounds that cannot be removed from the filter during regeneration. Although the ash accounts for only 1% of the engine-out PM by mass,²² after 150,000 miles of operation the ash can constitute as much as 80% of the matter trapped in the filter.²³ As seen in Figure 2-4, ash builds up both along the wall of the filter and as a plug at the outlet. The buildup of ash serves to increase the obstruction of exhaust gas flow thereby increasing the backpressure in the filter causing a reduction in fuel economy. To combat this, the filter must be regularly serviced to remove the ash. The increase in pressure drop is well documented, and continues to be an active area of research; this study, however, will focus on the effect of the ash on the catalytic activity of the filter, which could compromise the ability of the filter to passively regenerate soot.

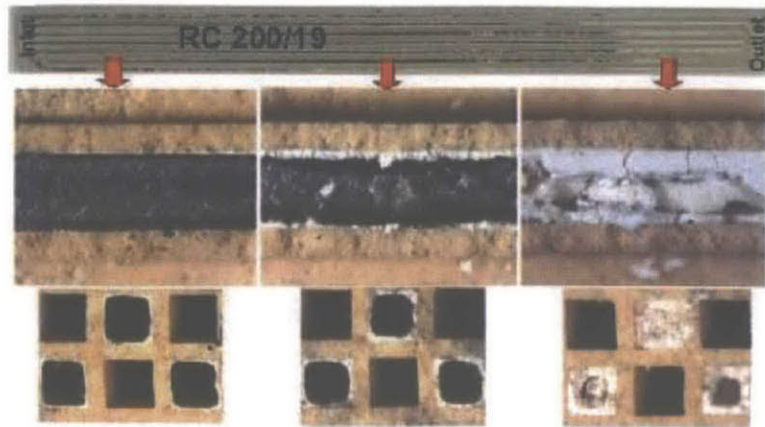


Figure 2-4 Ash and Soot Buildup in a DPF²⁴

2.3.1 Ash Sources

Almost all of the ash found in a DPF originates from lubricant additives that are necessary to ensure proper operation and durability of the engine. These additives are present in a number of different forms: detergents, dispersants, anti-oxidants, anti-wear additives, and friction modifiers. They are commonly magnesium (Mg), calcium (Ca), and zinc (Zn) based which end up as ash in the form of sulphates, phosphates, or oxides.²⁴ In an effort to minimize the amount of ash that is introduced to the system, limits have been placed on the acceptable level of sulfated ash (1.0%), phosphorous (0.12%), and sulfur (0.4%) content in lubrication oils.²⁵

The most significant mechanism in the transfer of ash compounds from the lubricating oil to the DPF is through the power cylinder. A small layer of oil is swept up past the piston rings into the cylinder where it is oxidized during combustion. In addition to being the major pathway for ash transfer, this is also the major source of oil consumption in the engine. The ash loading rate is proportional to engine oil consumption; however, it is less than would be predicted by the ash content of the oil alone. Ash capture efficiencies have been reported in literature between anywhere from 5 to 65%,^{24, 25, 26, 27} and are dependent on both the composition of the oil and the engine itself. The variations can be attributed to two major factors: first, the ash containing additive compounds are less volatile than the base oil and are therefore less readily reacted, and second, some of the ash will deposit on the exhaust stream components upstream of the DPF.

In addition to the lubricant derived ash, there are several other sources of particulate matter that may end up in the DPF. Iron and other metallic compounds resulting from engine wear or rust

can be entrained in the exhaust flow, as can fragments of the upstream DOC washcoat, substrate, or even its catalyst particles.^{22, 28}

2.3.2 Ash Transport

Ash enters the DPF bound to the soot particles as small precursors which have been observed in different size ranges, all significantly smaller than soot.^{29,30} Over the course of even a single regeneration event, the precursors are brought together and combine to form primary particles, which are reported to be an order of magnitude greater in size ($0.5\text{-}2\ \mu\text{m}$).²² Over time these primary particles continue to agglomerate, resulting in large ash particles as large as $5\text{-}50\ \mu\text{m}$.²²

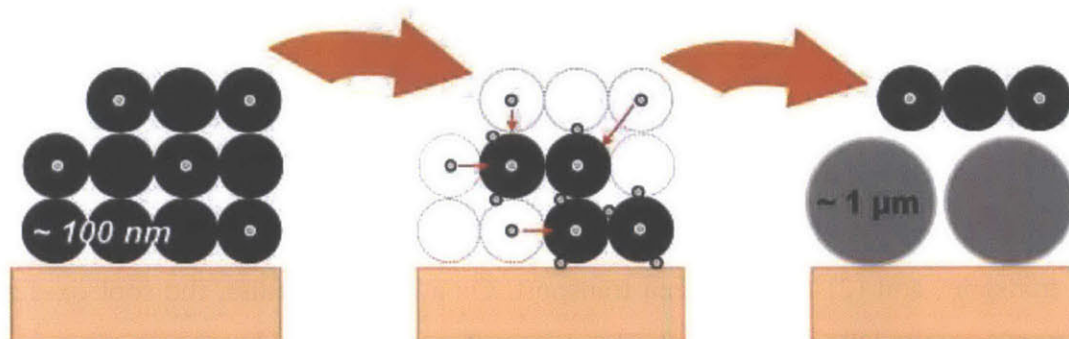


Figure 2-5 Schematic Representation of Ash Particle Formation and Growth over Repeated DPF Regeneration²⁹

As observed in Figure 2-4, the ash is deposited both as thin layer along the wall of the filter as well as a plug on the outlet side. A 2011 study used additive tracers to show that the buildup of ash, in both the wall layer and plug, is deposited in stratified layers.³¹ Figure 2-6 illustrates the distribution of ash in a DPF over time. Initially the wall layer builds up fairly evenly over the entire available surface area of the filter. Once a layer of critical thickness is attained ash is preferentially swept to the rear of the filter where it forms the plug.

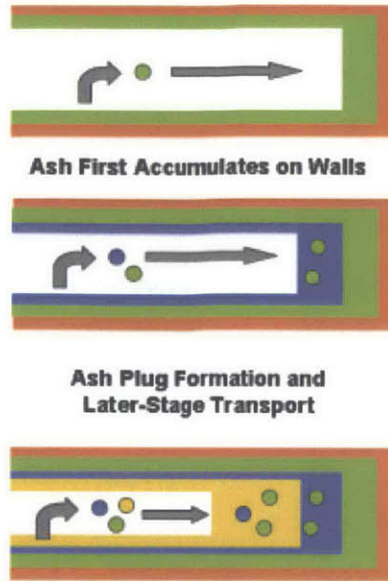


Figure 2-6 Conceptual Illustration of Ash Distribution in a DPF over Time³¹

Two primary factors result in the mobility of ash from the wall layer to plug: (1) regeneration induced transport, and (2) flow induced transport. On a catalyzed filter, the soot oxidizes from the side nearest to the DPF wall inward. This means that the soot that has the greatest contact and adhesive forces with the DPF wall is removed first, leaving behind soot that is less strongly bound to the surface. As these adhesive forces lessen, it becomes easier for the remaining soot to be entrained by the flow and transferred to the rear of the filter. This is the cause of regeneration induced transport. Flow induced transport is the result of elevated exhaust speeds that increase the shear force on the soot particles beyond the forces holding the particles in place. Both of these mechanisms have been observed to result in PM transport from the wall layer to the rear of the filter.³² Recent literature indicates that the thickness of the soot layer at the commencement of regeneration plays a large role in determining the mobility of the soot and ash. If the layer is thin, the PM is more likely to remain adhered to the rough surface of the DPF, and thus it is expected that a larger soot layer during regeneration would result in a larger ash plug.³²

2.3.3 Effects of Ash on DPF Pressure Drop

The addition of any obstruction to flow in the exhaust stream will result in a backpressure on the engine. In order to overcome that backpressure, the engine must expend usable work which could otherwise be used to produce the desired mechanical work output by the driveshaft. A DPF on its own produces a small backpressure, which hinders engine performance slightly, but the

effect is intensified by the presence of particulate matter. It is estimated that an increase of 10 kPa of backpressure could result in a decrease in fuel economy of 1.5-2.5% for a turbocharged engine and a 3-4.5% decrease in a naturally aspirated engine.³³

The pressure drop through a porous medium is governed by Darcy's Law (Eq. 2-3).

Eq. 2-3

$$\Delta P = -\frac{\mu}{kA} Q$$

Where,

ΔP = Pressure drop (backpressure)

μ = Fluid viscosity

k = Permeability

A = Filter area

Q = Volumetric flow rate

Both the ash layer and the plug serve to increase the pressure drop across the filter. The ash layer penetrates and blocks pores reducing the permeability (k) of the DPF substrate and therefore increasing the backpressure. It also creates a porous layer through which the flow must pass. The ash plug entirely fills the end of each channel which reduces the effective volume of DPF. Essentially the DPF is made shorter by the length of the plug, reducing the filter area (A) through which the exhaust gas flows.

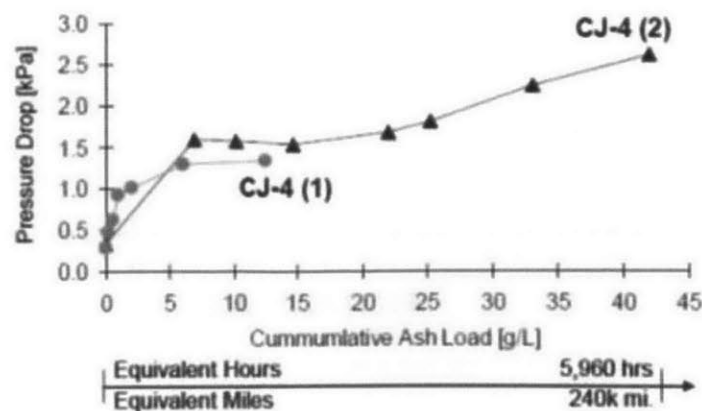


Figure 2-7 Effect of Ash on DPF Pressure Drop³⁴

Figure 2-7 depicts the backpressure response of a DPF to increasing ash load up to a simulated 240,000 miles. Two samples were aged using an accelerated aging apparatus under using periodic active regeneration conditions using standard CJ-4 certified oil.³⁴ The initial steep increase in pressure drop is the result of deep-bed penetration of the ash. After roughly 5 g/L of ash has accumulated on the filter there is no longer any penetration of the DPF pores, and the wall layer begins to form. Beyond this point the backpressure slowly increases as both the wall layer thickness and the plug length grow.

The addition of ash can both increase and decrease the pressure drop across the DPF depending on the extent of the ash load, as seen in Figure 2-8. At a low ash load the pressure drop resulting from soot accumulation is less than that of the clean filter.²⁹ This occurs because the ash has already started to form a porous layer which, in itself, acts as a filter. As a result the soot cannot penetrate the pores of the DPF substrate, thereby stopping any deep-bed penetration. Since ash is composed of larger agglomerate particles it has a higher porosity and a lower packing density than the soot. Therefore, filling the surface pores with ash instead of soot translates to a comparative reduction in pressure drop. In contrast, the backpressure experienced at a high ash load resulting from soot is greater than that of the clean filter. This occurs because as the ash layer and plug continue to grow, their effects continue to increase until they are more dominant than the reduction of pressure drop due to the lack of deep-bed penetration.

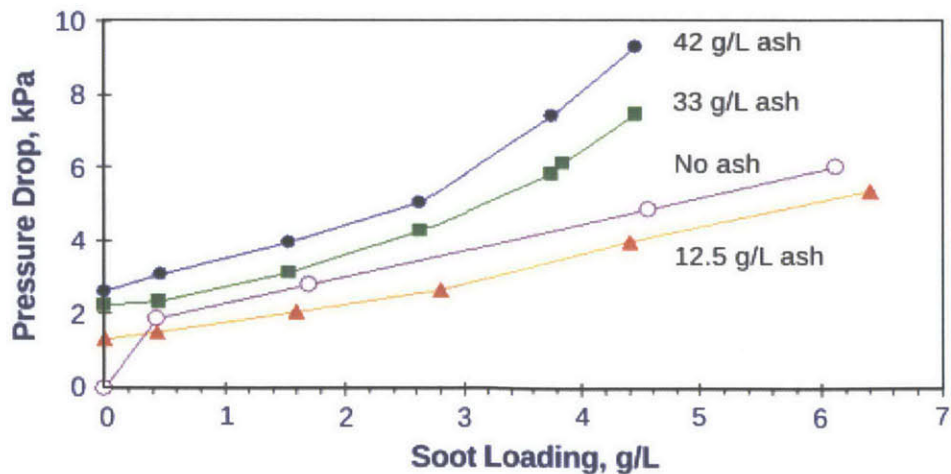


Figure 2-8 Effect of Soot and Ash on DPF Pressure Drop²⁹

3 DPF CATALYTIC ACTIVITY

Most modern diesel particulate filters utilize both passive and active regeneration to ensure total oxidation of the trapped carbonaceous soot. In a typical system the exhaust gas temperature is maintained throughout the DPF such that passive oxidation of the soot will occur continuously; however, due to fluctuations in the operating conditions of the system that may result in more soot being generated than can be continuously oxidized, periodic active regeneration is also employed when a sufficiently large pressure drop is measured across the filter, or after a predetermined number of miles driven.

The purpose of this study is to consider the effect of ash on the ability of the catalyst to carry out passive oxidation of soot. If the effectiveness of the catalyst is compromised, it would increase the speed at which PM is built up in the filter, causing the backpressure to increase at a faster rate, and resulting in the need for more frequent active regeneration events. Both of these consequences result in a direct fuel penalty.

3.1 CATALYST FUNDAMENTALS

A chemical reaction can be accurately described by the Arrhenius Equation (Eq. 3-1), which relates the rate of a reaction (k) to the temperature (T). It is also dependent on the pre-exponential factor (A), which is an empirically derived factor having the same units as the rate constant (s^{-1} for a first order reaction). The pre-exponential factor is related to the frequency with which the molecules undergoing reaction will collide, and the likelihood that during a collision they are in the necessary orientation to react. The activation energy (E_a) is a measure of the required energy that must be overcome in order for a reaction to proceed. This energy threshold is dependent on the total reaction mechanism, i.e., the series of elementary reactions that occur during the global reaction from initial reactants to final products.

Eq. 3-1

$$k = A e^{-\frac{E_a}{RT}}$$

Where:

k = Reaction rate constant

A = Pre-exponential factor

E_a = Activation energy

\tilde{R} = Universal gas constant

T = Temperature

A catalyst is any material that alters the rate of a chemical reaction without being consumed or produced.³⁵ Catalysts are said to be homogeneous if they are in the same phase as the reactants and heterogeneous, as in a DPF, if they are in different phase. A positive catalyst will speed up reactions by reducing the activation energy of the reaction mechanism as represented graphically in Figure 3-1. In the presence of a catalyst, the series of intermediate steps undergone during the overall global chemical reaction is altered such that less input energy is required to cause the reaction to proceed. When used in a DPF, this means that less fuel energy needs to be consumed in order to drive the reaction forward. Catalytic activity is used to describe a catalyst's ability to increase the rate of a given reaction; the more a catalyst increases the reaction rate the more active it is said to be.

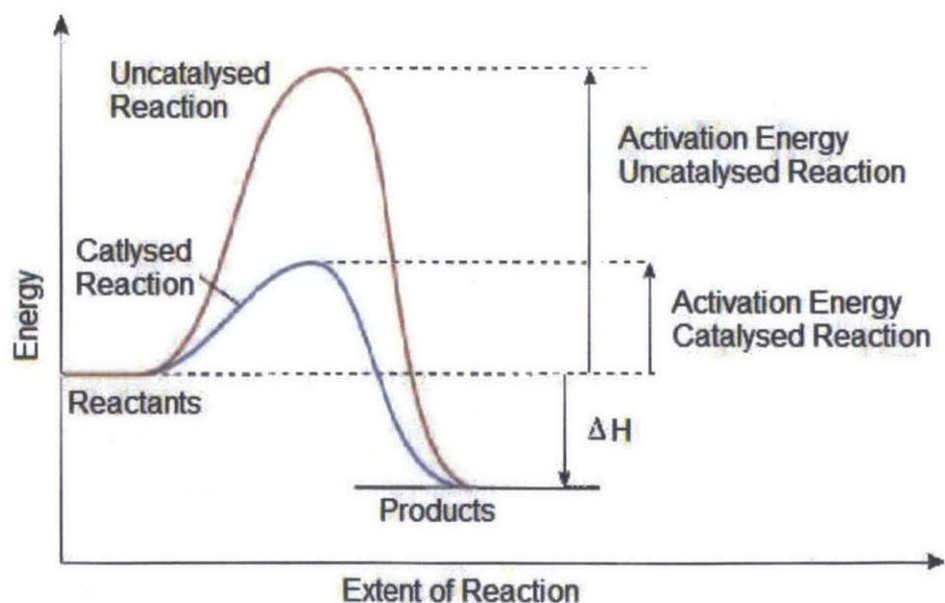


Figure 3-1 Effect of Catalyst on Activation Energy³⁶

A substance's interaction with a heterogeneous catalyst occurs in three intermediate steps: (1) adsorption onto the catalyst surface, (2) chemical reaction, and (3) desorption. Each of these steps requires a different amount of input energy in order to proceed. The step with the highest necessary energy is the "rate limiting step," which is the major factor determining the rate of

reaction. The apparatuses used in this research, which will be described in *Section 4*, were not equipped to distinguish between these different phenomena, and so the results generated represent only the combined effect of these three steps.

3.2 DPF Catalysts

As described briefly in *Section 2.2*, DPFs utilize catalysts to reduce the required energy needed to oxidize the soot collected within them. Although fuel-borne catalysts in the form of vanadium oxide, ceria or iron oxide have been used in some instances, the vast majority of passive emission control systems employ solid phase catalyst particles that are deposited on the washcoat layer, typically comprised of Alumina (Aluminum Oxide Al_2O_3) that coats the filter substrate. The function of the washcoat is twofold: (1) it controls the porosity of the substrate and (2) it increases the filter surface area, enabling the best dispersion of catalyst particles. The catalyst is dispersed as very fine particles in order to maximize the available active catalyst surface area for a given mass of catalyst used. Small particles are desirable because the ratio of surface area to volume increases as the particle size decreases.

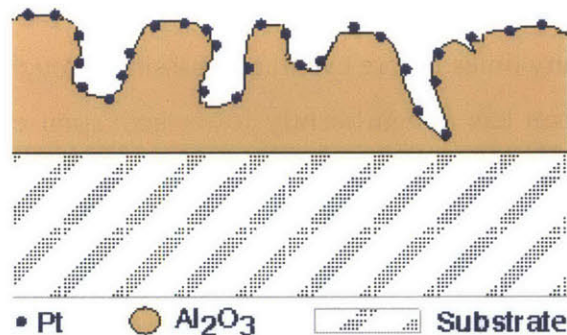


Figure 3-2 Pictorial Representation of Catalyst Distribution on a DPF Surface³⁷

DPF catalyst particles are most commonly made of platinum (Pt), which is highly active in the oxidation of soot as well as of CO and HC. Other platinum group metals, such as palladium, rhodium, and ruthenium, have been used as a substitute, but their usage is rare. In addition to their extremely high cost and tendency to sinter, a major drawback of PGM catalysts is their propensity to produce sulfate particulates that can poison the catalyst. This was the major factor that motivated the switch to ultra-low sulfur diesel, which has effectively solved the sulfur poisoning problem. Base metals like Vanadium, iron, and copper have also been employed as

DPF catalysts, particularly before the introduction of ULSD, because they do not produce sulfates; however, they are significantly less active than PGM catalysts in the oxidation of soot.³⁸

3.3 Catalyzed Oxidation of Soot

As described in *Section 1.1.3*, the two largest components of engine out PM emissions are carbonaceous soot and the SOF. The first catalyzed oxidation of this material occurs upstream of the DPF in the DOC. There, the Pt catalysts are able to convert almost all of the SOF, which is significantly more volatile than the carbonaceous soot. As a result, the particulates that deposit within the DPF are almost entirely elemental carbon.

The primary mechanism for the catalytic oxidation in DPFs is through the use of gaseous NO₂. NO_x molecules in the exhaust are converted from NO to NO₂ on the Pt catalyst surface and upstream in the diesel oxidation catalyst (DOC), enabling the oxidation of the carbonaceous soot via the chemical reaction described by Eq. 2-2. As depicted in Figure 3-3, the NO to NO₂ conversion occurs on the catalytically active sites and then back diffuses against the direction of bulk flow to reach the soot molecules. Once the NO₂ is converted back to NO it may cycle back to the catalyst to undergo the same reaction again. It is theorized that a single NO_x molecule may be recycled in this way many times before eventually passing through the filter. As expected soot oxidized via this mechanism has a significantly lower activation energy (39-60 kJ/mole) than that of uncatalyzed oxidation using oxygen (105-207 kJ/mole).^{39,40,41}

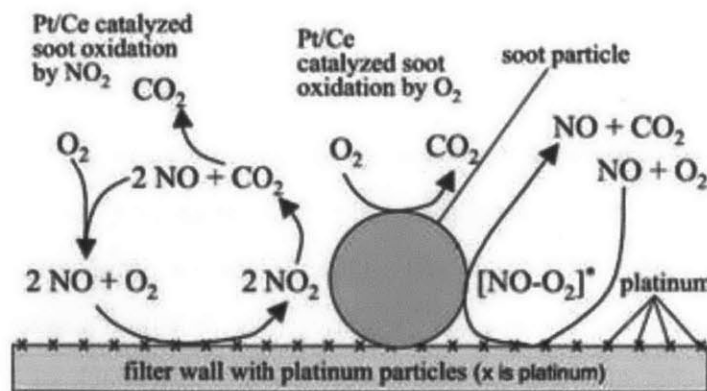


Figure 3-3 Illustration of Catalyzed Oxidation of Soot⁴²

Another mechanism for soot oxidation is the oxygen spillover reaction, also depicted in Figure 3-3.¹⁹ An oxygen molecule is able to dissociate on the catalyst surface, and then each individual oxygen atom can then be transferred to the soot particle where it will react to form CO and CO₂.

A recent study has shown that this mechanism requires direct contact between the soot and catalyst particles in order for the reaction to occur.⁴³ In an oxygen rich environment without any NOx carbon failed to oxidize when separated from the catalyst by a thin non-reactive substance.⁴³ When the interface between soot and the DPF washcoat is observed, as in Figure 3-4, a clear physical separation is visible. Since the soot and catalysts do not maintain direct contact, the oxygen spillover mechanism will likely contribute very little to soot regeneration.

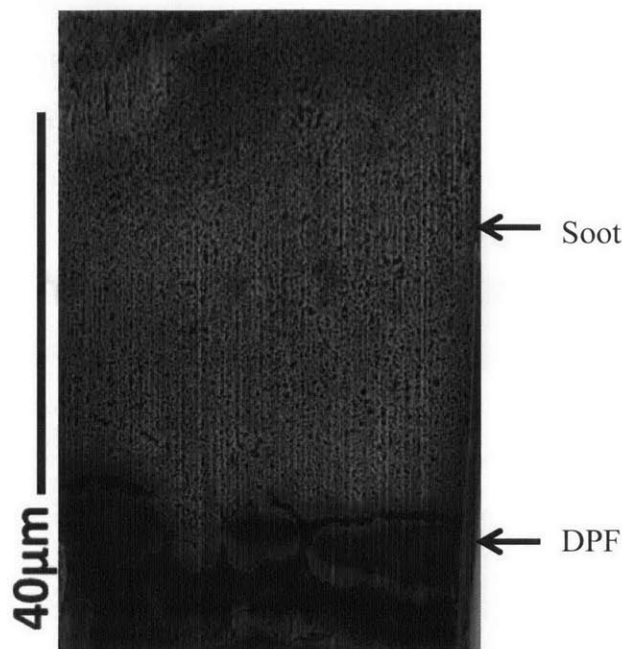


Figure 3-4 SEM Image of Soot-DPF Interface⁴⁴

3.4 Modes of Catalyst Deactivation

The deactivation modes of a solid particle catalyst can be divided into two primary mechanisms: the covering or masking of active sites through the introduction of outside material and the changing of the catalyst/substrate surface resulting from thermal aging. Both of these modes are prevalent in a DPF, and play an important role in its ability to effectively regenerate over its lifetime.

3.4.1 Catalytic Deactivation through Physical Masking/Poisoning

Foreign material that deposits in a DPF can deactivate the catalyst either selectively through chemical poisoning or nonselectively by physically masking (fouling) the catalytically active sites. Each of these modes is depicted in Figure 3-5.

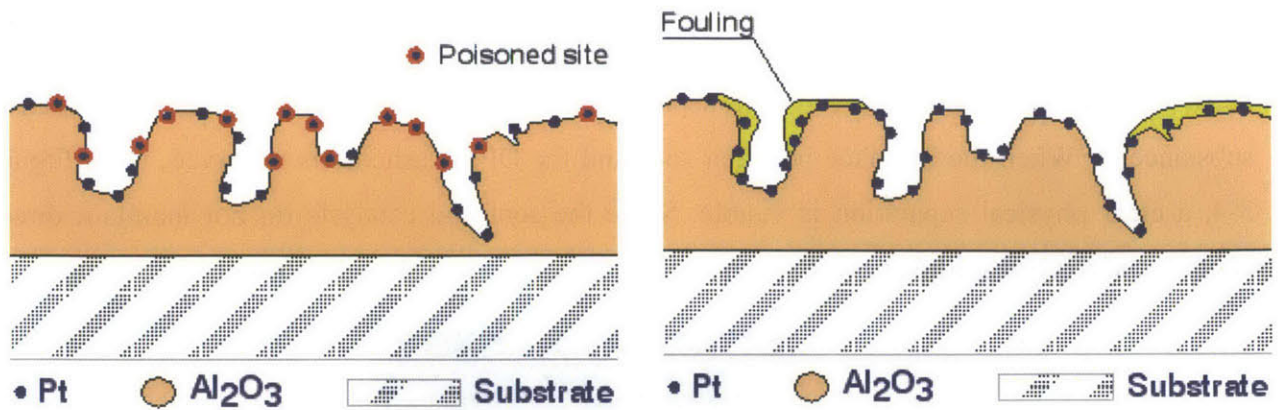


Figure 3-5 Illustration of Catalytic Deactivation via Poisoning/Fouling³⁷

Selective deactivation occurs when a chemical reacts directly with the catalyst and inhibits its ability to promote the desired reaction. Some metals, like lead and mercury, will react with platinum to form an alloy that has no beneficial catalytic ability. Once created it is very difficult to reverse the process, so the alloyed platinum will remain inactive throughout the lifetime of the filter. Other compounds, like phosphorus and sulfur dioxide (SO₂), can adsorb onto the catalytically active sites making them inaccessible for further reaction. Poisoning of this sort is reversible; the chemicals can be forced to desorb from the surface through heat treatment or washing.³⁷

Nonselective deactivation is the result of compounds indiscriminately depositing on top of the catalyst. Although the catalyst particles remain chemically active, they are rendered useless if there is a physical barrier preventing the exhaust gas from reaching their surface. Fouling due to the deposition of material can cover the catalyst particles directly and also block the pores causing the platinum within the pores to become inaccessible.

3.4.2 Catalytic Deactivation through Thermal Aging

At high temperatures the structure of both the catalyst particles and the washcoats on which they are deposited can change. This process is referred to as sintering and it can alter the effectiveness of a catalyst. An illustration of the effect is provided in Figure 3-6.

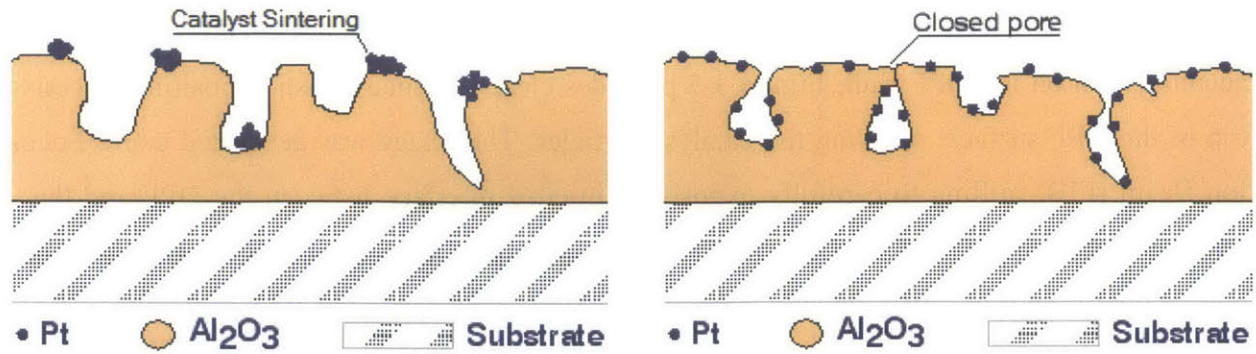


Figure 3-6 Illustration of Catalytic Deactivation through Thermal Aging³⁷

When catalyst particles sinter they tend to agglomerate. As they combine there is a reduction in the total available catalyst surface area. In general, this will result in a loss of catalytic activity since the chemical reactions occur only on the surface of the particles.³⁷ Moreover, thermal aging will also alter the structure of catalyst particles, which in some cases can lead to an increase in the number of available catalytically active sites on the surface. Pt has several stable surface atomic configurations such as (101) and (111) which have different concentrations of Pt atoms per surface area. A switch between these states could lead to a change in catalytic activity without a change in size of the particle. Further investigation is required to fully understand the impact of elevated temperatures on catalytic activity resulting from catalyst sintering.

The alumina washcoat will also undergo thermal aging. Over periods of elevated temperature the washcoat will expand and shift causing its internal pore structure to change. In addition to increasing the restriction to flow of exhaust gas, this can also cause some surface pores to close entirely, isolating any catalyst particles they may contain from the flow. The trapped catalyst particles will be unable to participate in any chemical reactions and are therefore effectively deactivated.

3.5 Effects of Ash Accumulation on DPF Catalysts

The catalysts in a DPF will experience aging resulting from both poisoning and thermal sintering due to the extreme cyclic environments typically experienced by the catalysts/filters. This study primarily considers the effects of the buildup of ash in the filter on the catalyst, neglecting the thermal effects. A study into the effects specifically resulting from thermal aging would constitute a positive extension on the results found in this study and contribute positively to the current understanding of the effectiveness of DPF catalysts over their entire usable lifetime.

Using scanning electron microscopy (SEM) one can directly observe the modes of ash accumulation on the DPF wall. Figure 3-7 provides clear evidence of ash depositing directly on top of the DPF surface, masking the catalyst particles. The image was generated using Focused Ion Beam (FIB) milling to carefully expose the internal interface between the DPF and the ash without disturbing it.⁴³ One can observe both a very thin ash layer that coats the DPF surface, as well as a larger porous layer which constitutes the bulk of the deposited ash.

The ash was found to be comprised primarily of calcium, phosphorus, and sulfurⁱ throughout its entirety. Knowing the chemical composition of the ash and its temperature history, it was assumed that the thin coating was mechanically, not chemically, bound to the surface.⁴⁴ This suggests that ash deposits result in noticeable nonselective catalyst poisoning.

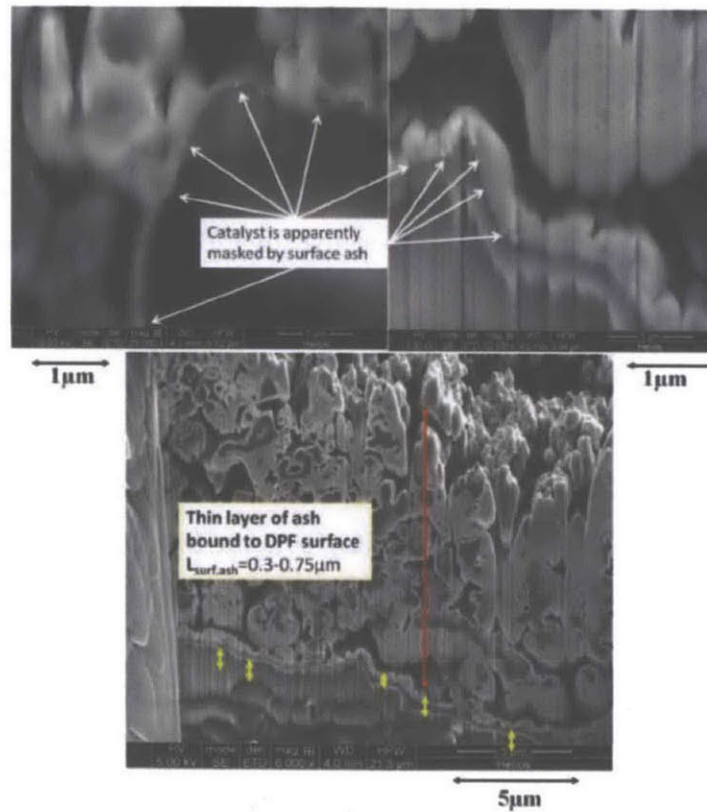


Figure 3-7 SEM Image of Ash Coating Catalyst Particles⁴⁴

In addition to the masking of catalyst particles due to an ash layer coating, the porous wall layer also serves to reduce the ability of the filter to regenerate soot. Figure 3-8, which was similarly

ⁱ The lubrication oil used during the aging of this sample contained primarily calcium based additives. This explains the lack of any magnesium or zinc as would be expected if regular CJ-4 oil was used

prepared using FIB milling, shows that the ash wall layer forms a physical barrier separating the DPF surface and the soot. This is a porous layer through which the exhaust gas is able to flow, but since the catalyst is deposited on the DPF surface, the NO_2 generated must back diffuse from the DPF wall to the soot through the ash. As this layer increases it may reduce the amount of NO_2 that is able to reach the soot, and therefore reduce the ability of the filter to regenerate. This effect is not the result of catalytic deactivation, since the catalyst is still able to promote the conversion of NO to NO_2 , but it will have an impact on soot conversion nonetheless.

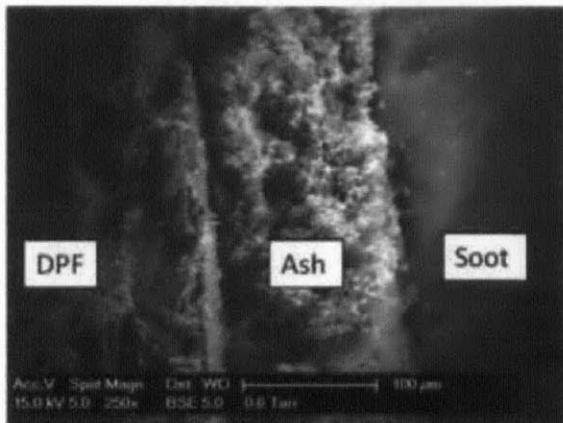


Figure 3-8 SEM Images of Stratified DPF-Ash-Soot Layers⁴⁴

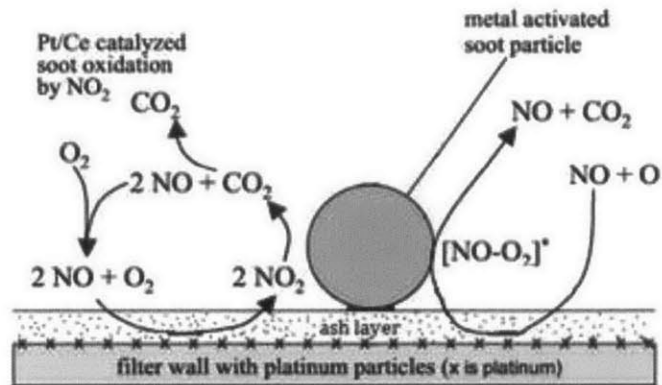


Figure 3-9 Illustration of Ash Layer Impact on Catalytic Reaction⁴²

As discussed in *Section 2.3.2*, ash builds up both as a layer along the full length of the channel walls as well as a plug at the outlet side of the filter. Figure 3-10 is an X-Ray computed tomography (CT) image of a filter loaded to 42 g/L on an accelerated aging system intended to simulate 240,000 miles of operation (this sample will be discussed in more detail in *Section DPF Ash Loaded Samples*). The ash plug is clearly visible, and makes up roughly 32% of the filter volume. The plug section of the filter is essentially inaccessible to the flow of exhaust gas, which prevents the catalyst particles trapped in the plug from participating in any useful reactions.

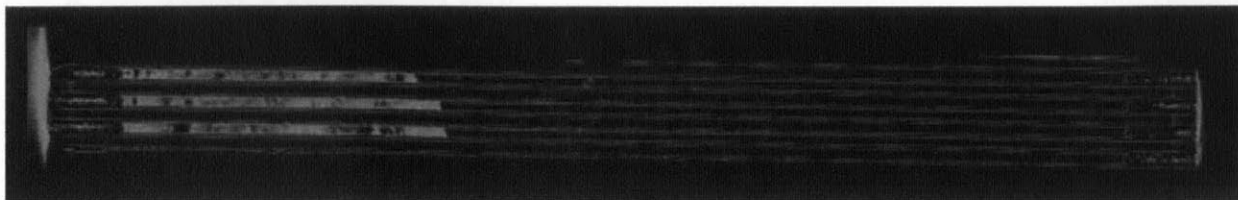


Figure 3-10 X-Ray CT Image of DPF Core Sample

In addition to the ash plug's direct fouling behaviour, it causes several secondary effects. Since the filter volume is effectively reduced, the flow through the wall of the filter must increase proportionally. A higher flow velocity translates to a lower residence time for the exhaust gas flowing through the filter. Consider a single NO_x molecule as it passes through the flow: if its velocity is increased it has less time to react with the catalyst or the soot which translates into slower regeneration. Also, any increase in flow velocity will increase the resistance to molecular back diffusion. Since catalytic soot oxidation is driven by the NO₂ that is transferring through the ash layer opposing the bulk flow direction, any increase in back diffusion resistance will reduce the fraction of NO₂ generated that is able to reach the soot. Altogether this means that the ash plug will both limit the DPF catalyst's ability to produce NO₂, as well as make it more difficult for the NO₂ molecules to diffuse against the flow to reach the soot layer.

4 EXPERIMENTAL SET-UP AND TECHNIQUES

Over the better part of the last decade researchers within the Sloan Automotive Lab at the Massachusetts Institute of Technology (MIT) have studied the effects of ash accumulation on DPF performance. As a fundamental part of their research they have developed a variety of experimental techniques designed to simulate the accumulation of ash and analyze the impact of particulate matter on DPFs. In addition to the data their experiments produced, they compiled a library of laboratory aged DPF samples that had been generated as part of various projects targeting specific aspects of ash composition and DPF operation.

The research presented in this thesis builds on the results of those earlier experimental studies by looking specifically at the impact ash has on catalytic activity and the oxidation of soot. The DPF samples used in this study were previously aged by Dr. Alex Sappok while he was a graduate student at MIT.⁴⁵

This section will outline the procedures under which those DPF samples were generated and the experimental apparatuses used in this study to specifically target catalyst performance.

4.1 Accelerated Ash Loading System

As discussed in *Section 2.3*, the buildup of ash occurs gradually over the entire lifetime of the filter. While field-aged samples provide useful insights into the aging process, the inherent variability of on-road operating conditions adds a measure of significant complexity to the ash deposition process. In order to study the long-term effects of ash accumulation it was necessary to generate a series of carefully aged DPF samples, each aged in a manner that would reflect real life operating conditions and permit the controlled investigation of the effect of individual variables upon the filter. Aging each sample under laboratory conditions using only regular engine out emissions would have been prohibitively expensive and time consuming. The only reasonable alternative was to create a laboratory based system that would accurately simulate, within a reasonable timeframe, realistic loading conditions on the DPF. .

The accelerated ash loading system developed at MIT is represented schematically in Figure 4-1. Its operation and validity have been described in detail in previously published literature.⁴⁶ The system was designed to replicate in-cylinder combustion of lubrication oil, as described in

Section 2.3.1, through the injection of oil directly into a self-sustained flame generated with diesel fuel by a commercial burner. The flow of this ash-rich exhaust is driven by a centrifugal blower, and forced into a heat exchanger before passing through the DPF.

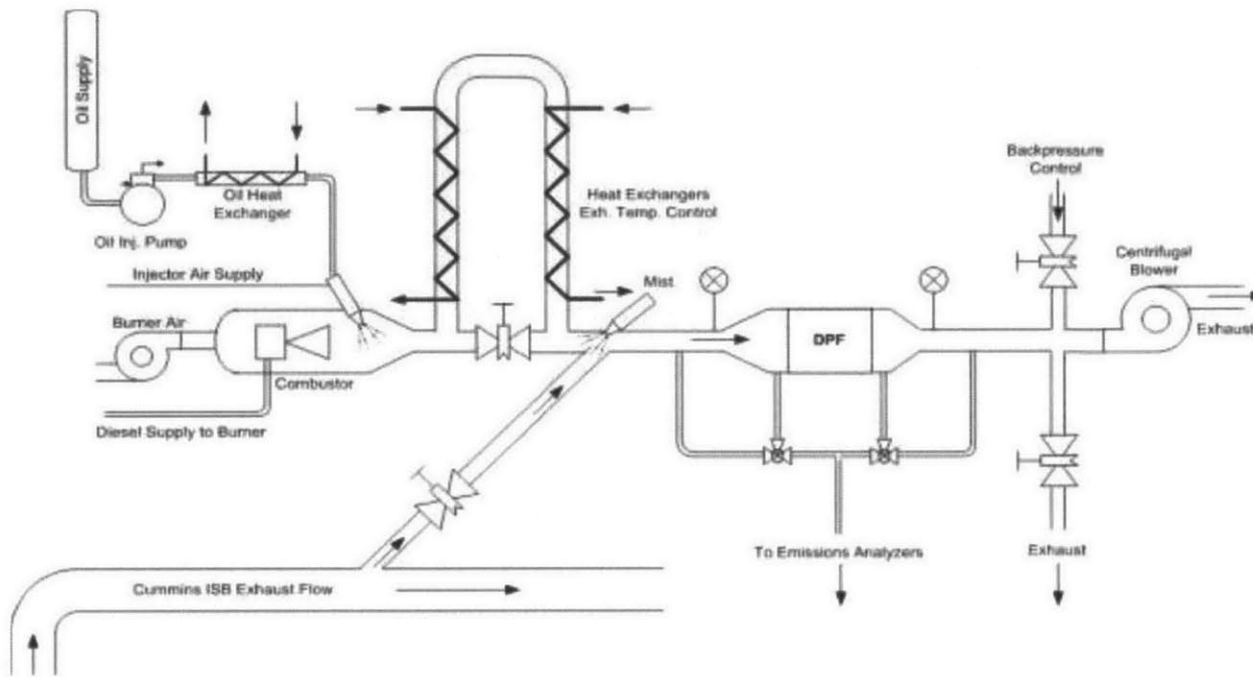


Figure 4-1 Schematic of Accelerated Ash Loading System²³

The heat exchanger allows precise control of the exhaust gas temperature, which is measured directly using thermocouples just upstream and downstream of the sample. The exhaust flow rate is controlled either by adjusting the speed of the centrifugal blower or by opening/closing the backpressure control valve. Oil flows into the system through an air-assisted injector nozzle which atomizes the lubricant to ensure adequate combustion within the diesel flame. The rate of ash accumulation can be controlled by adjusting the rate of oil injected with a computer controlled constant volume pump. The possible ranges of operation for the relevant loading parameters are summarized in Table 4-1.

Table 4-1 Accelerated Ash Loading System Parameter Specifications⁴⁵

System Parameter	Specification
Fuel Consumption	1.5 - 7.6 [L/h]
Oil Consumption	0.94 - 9.4 [mL/min]
Injection Pressure	700 - 1400 [kPa]
Air Flow	266 - 1130 [SLPM]
DPF Inlet Temperature	200 - 800 [°C]

In addition to simulating ash generation that results from oil passing past the piston ring pack and into the combustion chamber where it combusts, the system is equipped with an oil mist injector that can simulate liquid oil losses that may result from valve and turbocharger seal leakage. Although the system is capable, the samples generated in this study did not utilize the oil mist system because oil leakage is a secondary source of ash that is much less significant than the piston ring pack mechanism.

4.2 DPF Ash Loaded Samples

Over the course of this study several different DPF samples were analyzed in an effort to understand the effects of ash on DPF catalytic activity. All of the samples were identical standard cordierite filters with a diameter of 5.66” and a length of 6”. The cells (channels) of each filter were packed with a density of 200 cells per square inch and had a wall thickness of 0.012”. Each of the filters had an Alumina washcoat and platinum catalysts.

The filters were aged using periodic regeneration. The inlet temperature of the filter was maintained between 200°C and 250°C during regular operation and then spiked to 600°C at the end of every hour of loading in order to facilitate regeneration. Based on the temperature profile used during the aging process, one can reasonably assume that the oxidation of almost all of the soot occurred via the active O₂ reaction mechanism.

The ULSD fuel used in the accelerated aging burner system underwent elemental analysis. The results of this test (ASTM D5185) are presented in Table 4-2.

Table 4-2 Elemental Analysis of the Test Fuel⁴⁵

ASTM D5185						
Element	Ca	Mg	P	Na	K	Zn
ULSD [ppm]	<97	<56	<1180	<2010	<2690	<155

The oil used to age the samples contained 1.0% sulfated ash content by weight and adhered to the CJ-4 standard. An elemental analysis of the oil was conducted using the ASTM D5185 test, the results of which are provided in

Table 4-3.

Table 4-3 Elemental Analysis of Test Oil⁴⁵

Lubricant	ASTM D5185							
	B [ppm]	Ca [ppm]	Fe [ppm]	Mg [ppm]	P [ppm]	Zn [ppm]	S [ppm]	Mo [ppm]
CJ-4	586	1388	2	355	965	1226	3200*	77

The amount of ash accumulated inside the DPF was measured directly by weighing the DPF at the end of each day of operation. In order to ensure that no water vapor has condensed on the DPF the sample was weighed while hot (>100 °C). The increase in weight due to ash accumulation can be directly correlated to the number of miles of simulated operation. In order to carry out this calculation the following assumptions were adopted: (1) a typical medium heavy-duty diesel engine consumes oil at a rate of 15 g/hr, (2) a typical vehicle travels at an average speed of 40 mi/hr, and (3) a DPF installed on a full sized engine has a volume of 12 L.

In this study two ash loaded DPFs were compared to a clean unused sample. These filters are detailed below in Table 4-4.

Table 4-4 Laboratory-Aged DPF Sample List

Substrate	Ash Load (g/L)	Equivalent Loading (miles)	Regeneration Mode	Ash Layer Thickness (mm)
Catalyzed Cordierite	0	0	N/A	0
	12.5	72,000	Periodic/Active	0.06-0.08
	42	240,000		0.12-0.18

The ash layer thickness was measured as part of the post-mortem analysis of these filters. Several core samples were cut from the filter in the axial direction (parallel to the channels) and then sectioned into four 1.5” length segments as outlined in Figure 4-2. The face of each segment was photographed, and the thickness of the ash layer was measured using image processing. Segmenting the filters in this way enabled the measurement of the distribution of ash both axially along each channel as well as radially outward from the filter centerline.

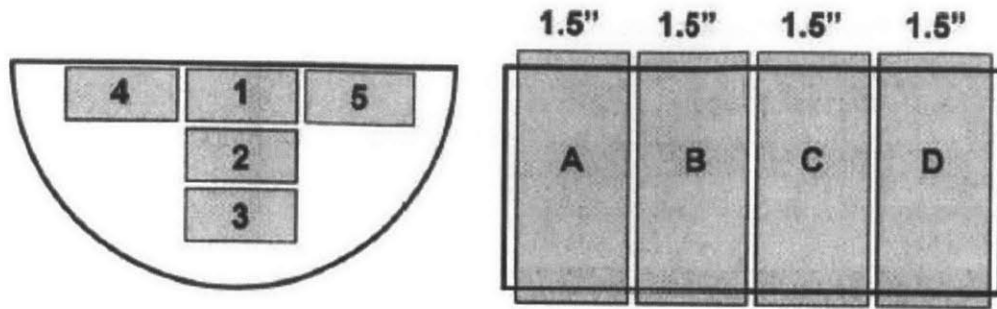


Figure 4-2 Illustration of DPF Core Sample Geometry⁴⁵

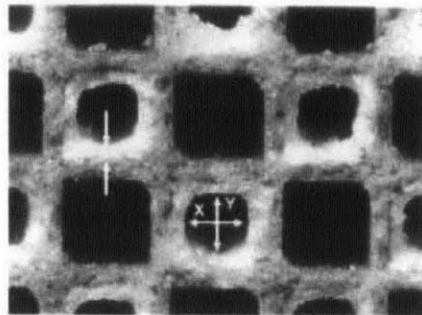


Figure 4-3 Close-up Image Used to Measure Ash Layer Thickness⁴⁵

The distribution of ash in the fully loaded DPF sample can be seen in Figure 4-4. Once established, the ash layer thickness remains fairly constant until it reaches the plug at the rear of the filter. It is also interesting to note that, although there is not a huge radial variation in the ash distribution, the plug is largest at the center of the filter and becomes smaller towards the edge.

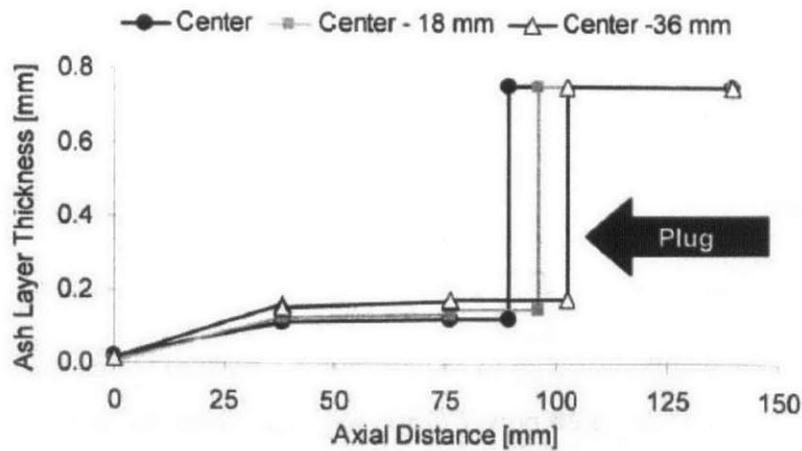


Figure 4-4 Ash Layer Distribution in 42 g/L (280,000 mi) DPF Sample⁴⁵

To further study the catalytic activity of these filters, additional core samples were cut, again along the axial direction in line with the channels. It was desirable to use sections from as near to the centerline of the filter as possible to negate the effects of the fluid boundary layer caused by the wall of the filter housing. The core samples used were 7 by 7 channels, and were mounted in stainless steel tubes using intumescent matting. Figure 4-5 shows a selection of these samples in their final form in.



Figure 4-5 Canned DPF Core Samples

4.3 DPF Core Sample Soot Loading System

In order to test the ability of DPFs to regenerate soot at different levels of ash loading, it was necessary to load the core samples with PM in a realistic way. This was accomplished using a single cylinder Pramac Yanmar diesel generator. The specifications for the model used are given in Table 4-5.

Table 4-5 Pramac S5500 Yanmar L100V Generator Specifications

Model	Maximum Continuous Power	Maximum Surge Power	Aspiration	Displacement Volume	Compression Ratio
L100V	5.0 kW @ 3600 rpm	5.5 kW @ 3600 rpm	Natural	0.435 L	21.2:1

Load was applied to the engine using up to 4 space heaters, each of which are capable of drawing 30% of the engine’s maximum rated power (1500 W). Whenever the core samples were loaded with soot three of the four heaters were turned on to their full power in order to operate the engine at 90% of its capacity.

Since the DPF core samples were small, only a fraction of the exhaust put out by the diesel generator was necessary to fully soot load the sample. A schematic of the soot loading apparatus is provided in Figure 4-6. A centrifugal pump was used to pull exhaust through the DPF core sample. The pump operated at a constant speed, so the exhaust flow was maintained at the desired rate using a backpressure control valve. Flow through the DPF could be quickly started and stopped using a valve upstream of the DPF.

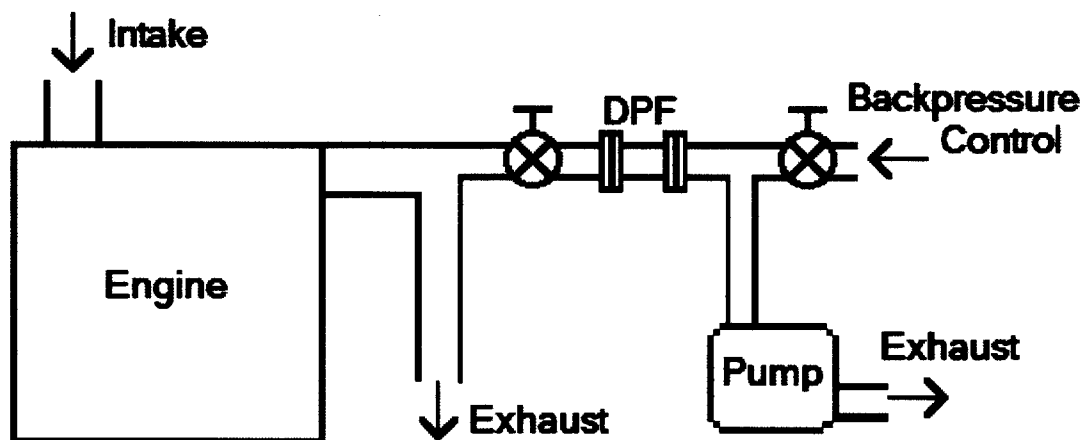


Figure 4-6 Schematic of DPF Core Sample Soot Loading Apparatus

The procedure for soot loading was as follows:

1. 5 minute idle period at 0% load
2. 5 minute warm up period at 90% load
3. 10-30 minute ash loading period (time dependent on sample used and desired soot load)
4. 5 minute cool down period

During steps 1, 2, and 4 the pump was turned off and the valve upstream of the DPF was closed. The weight of the core samples was measured before and after the loading of the soot. Any increase in weight could be attributed to the accumulation of soot as long as the filter temperature was maintained above 100°C to ensure no water condensed on the surface.

4.4 Catalyst Flow Bench Reactor

A small scale flow reactor was constructed to simulate the flow of exhaust through the DPF core samples. This apparatus is depicted schematically in Figure 4-7. The flow was generated using a collection of compressed gas bottles, each of which had its own flow controller enabling the

relative amount of each gas species that made up the simulated exhaust to be accurately controlled. Accordingly, the gas composition through the filter remained extremely consistent, resulting in very precise laboratory measurements.

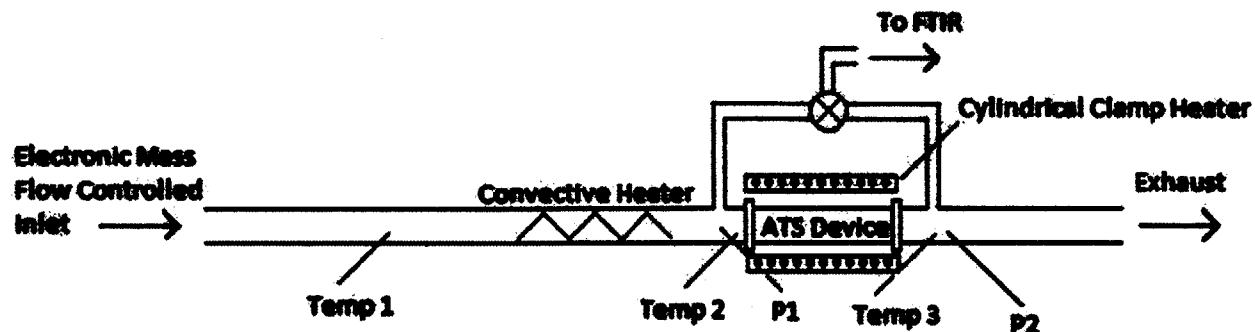


Figure 4-7 Schematic of Flow Bench Reactor

The flow passes through a convection heater, which can be set to maintain a constant temperature or programmed to increase the temperature at a selected rate from atmospheric conditions to 650°C within 1°C of accuracy. A cylindrical clamp heater is used to insulate the DPF in order to minimize the difference in temperature from the front of the filter to the back. Thermocouples are placed at several points throughout the apparatus, as labeled in Figure 4-7, in order to monitor the temperature response of the system.

Two thermocouples are placed inside the DPF itself: one 0.5” from the inlet face and one 0.5” from the outlet face. This arrangement enables the direct measurement of the internal temperature of the DPF. In order to accurately study the chemical interactions between the DPF catalysts and the exhaust gas it was essential to have a reliable internal temperature measurement. Figure 4-8 shows the difference in temperature between the front and back of the filter during several experiments in which reactions were taking place during a temperature ramp.

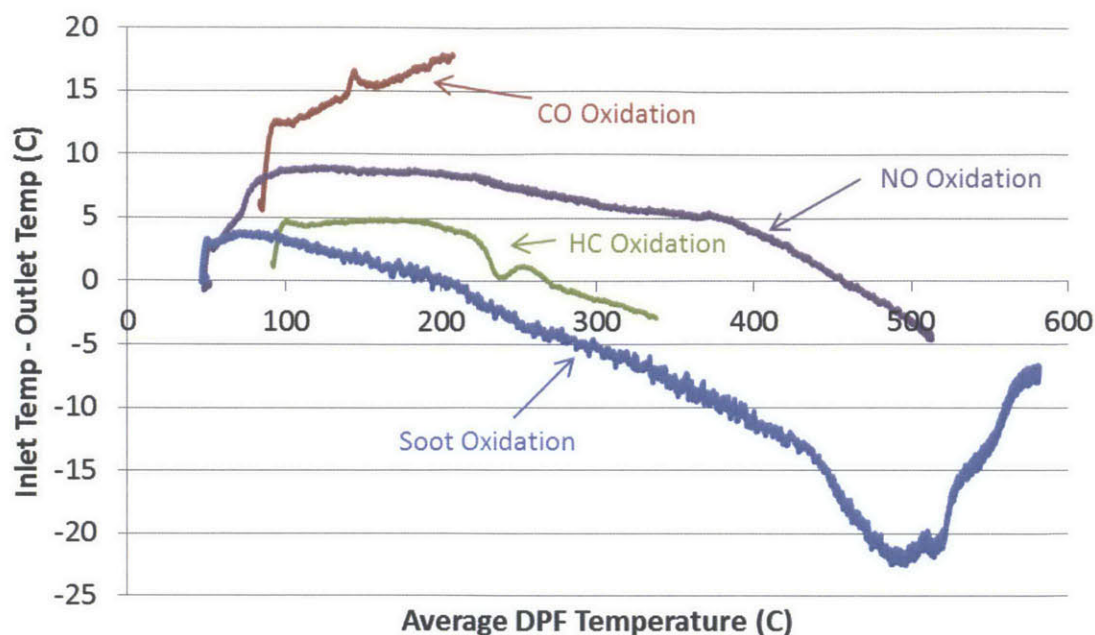


Figure 4-8 DPF Thermal Stability during CO, HC, and NO Oxidation

The difference in temperature during soot and CO oxidation was accurate within at least 20-25°C, and within 10°C during NO and CO oxidation. The rate of each of these reactions is highly dependent on temperature, and thus, the programmed ramp rate and thermal stability of the system were very important. The samples themselves, as described in *Section 4.2*, were housed in stainless steel tubes, which add significant thermal mass to the system, increasing the deviation in temperature from the front of the filter to the back. Each of these oxidation reactions is exothermic, which accounts for the increase in temperature at the rear of the filter at high temperatures. This is because the energy released during the reaction will be transferred to the exhaust gas, increasing its temperature. The exothermic effect is particularly evident during soot oxidation in which the rear of the filter becomes significantly hotter than the front. In all experimental results presented in *Section 5* the temperature reported is the average between the two internal thermocouples. Given the variation in temperature across the filter, caused by the thermal interaction of the steel tubes plus the exothermic nature of the reaction, an average was the most representative number that could be measured using this apparatus.

Sampling lines upstream and downstream of the filter are connected to an MKS MultiGas™ 2030 Fourier Transform Infrared Spectrometer (FTIR) Continuous Gas Analyzer, which was

capable of determining the gas phase composition of the exhaust stream with a sensitivity of 10-100 ppm.⁴⁷ The FTIR enables the direct measurement of the conversion of CO, HC, NO_x, and soot across the filter by comparing the composition of the gas on either side of the filter.

Pressure sensors were positioned on either side of the test section so that the pressure drop across the filter can be measured directly. Both an analog differential pressure sensor and two digital pressure transducers were installed allowing for double confirmation of the resulting data.

Because of the high toxicity of the gaseous species used in this apparatus the test section was enclosed in a fume-hood. As an extra safety precaution the system was also leak tested before every test.

4.4.1 Catalyst Flow Bench System Improvements

Several updates have been made to the flow bench system that were not utilized during this study, but which could be useful for further research into this subject. The primary additions were the introduction of water vapor into the exhaust stream to better simulate on-road conditions, and a bypass system which enables the flow to reach steady state conditions before the oxidizing gaseous species flow through the filter. The finished system is depicted in Figure 4-9.

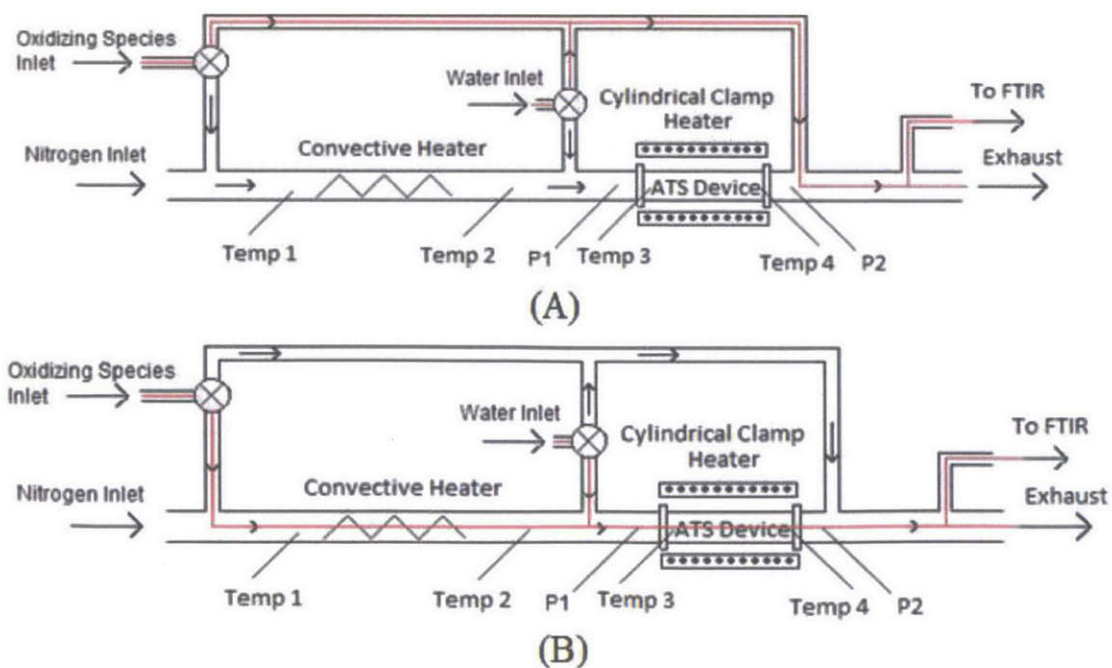


Figure 4-9 Updated Catalyst Flow Bench Schematic

In condition (A) both upstream valves are set to divert the flow of the oxidizing species (NO_x, O₂, etc.) as well as the water vapor around the test section leaving only unreactive N₂ to flow through the filter. In this mode of operation the concentrations of each gas species can be calibrated and the temperature throughout the ATS can be set without the catalyst on the filter being exposed to any reactive substances. When the valves are reversed, as in condition (B), all of the reactive gaseous species will enter the filter at the same instant at any desired temperature set point and flow rate. This enables accurate isothermal experiments in which it is critical to observe the experiment from the instant it begins.

Adding liquid water to the system could cause significant damage to the flow bench reactor, and would not be representative of actual engine exhaust. In order to supply a steady stream of water vapor, a syringe pump was used to slowly pump water into a coil of copper tubing. The tubing was wrapped in electrical heating rope which was then insulated with header wrap. In this way the vertical coil could be maintained around 160°C so that the water would instantly vaporize and pass up out of the coil into the test section as shown in Figure 4-9. Any liquid water that entered the coil would be held at its bottom by gravity.

Although these systems were installed, they had not undergone complete testing or analysis and therefore were not used and had no impact on the tests conducted or the results produced in this study.

The catalyst flow bench system could be further improved by adding solenoid valves between the compressed gas bottles and the intake manifold. The use of these solenoids would allow the flow to be pulsed, a feature that would provide a better representation of actual engine operating conditions and allow for the investigations of specific nonlinear phenomena that occur when the soot and/or other species are first met by oxidizing species.

(This page intentionally left blank)

5 EXPERIMENTAL TESTING AND RESULTS

The apparatuses and samples described in *Section 4* were used in this study to investigate the effects of ash accumulation on DPF catalytic activity. The main goal of this research was to determine if ash inhibits the ability of catalysts to oxidize soot and, if so, to identify the mechanisms through which the performance is reduced.

Each test described in this section was conducted at least twice to ensure the results obtained were repeatable.

5.1 Gaseous Conversion in the DPF

The primary purpose of a DPF is to minimize PM emissions, and it does so by capturing and destroying nearly all carbonaceous soot via oxidation (i.e., regeneration). The pressure drop over the DPF increases significantly during PM accumulation but is reduced during regeneration. Although soot oxidation is the most critical chemical reaction indicating proper DPF function, it is incredibly complex, making it difficult to determine the true impact of ash accumulation. By first measuring the effect of ash on catalytic activity during simpler gaseous reactions – specifically CO, HC and NO oxidation – the behavior of the filter during the regeneration of soot becomes easier to understand.

In order to test the gaseous conversion performance in various DPF samples, the catalyst flow bench system described in *Section 4.4* was used to simulate engine-out exhaust consisting of NO, CO, O₂, N₂ and HC in the form of propylene (C₃H₆). The ranges of typical concentrations for each of these oxidizing species are summarized in Table 5-1.⁴⁸ During every test O₂ made up 10% of the flow by volume, which is in excess of the amount necessary for oxidation. Previous research has shown that once the concentration of O₂ is greater than 1-2%, the addition of more O₂ has little impact on the chemical reactions in a DPF,⁴¹ and so a high concentration was selected in order to ensure the flow of simulated exhaust always represented lean combustion. NO, CO and HC were present in small amounts (usually 500 ppm) in order to be consistent with realistic engine operating conditions,⁴⁸ and the remainder of the gas was N₂. The details of the gaseous species concentrations, flow velocities, and temperature characteristics are summarized in Table 5-2 for each test presented in this section.

Table 5-1 Typical Concentrations of Diesel Engine Emissions⁴⁸

Gaseous Species	Concentration Range (ppm)
NO _x	50-1000
HC	20-300
CO	10-500

Due to the adsorption and desorption of molecules to and from the DPF and ash surfaces – a phenomenon that will be discussed further in *Section 5.1.3* – it was necessary to preheat the samples. Before each of the tests described in this section was conducted the samples were heated to over 600°C in pure nitrogen and held at that temperature until all of the gas species had desorbed from the sample. This procedure ensured a high level of consistency in the initial state of the system at the beginning of each test.

Table 5-2 DPF Gaseous Conversion Test Matrix

DPF Ash Load	Gaseous Species	Concentration	Temperature Characteristics	Flow Velocity	
g/L		ppm		hr-1	
0	NO + CO + HC	500	Ramp at 20°C/min	40,000	
42					
0					
12.5	CO				
42					
0					
12.5	HC				
42					
0					
12.5	NO		100	Ramp at 10°C/min	20,000
42					
0					
12.5		40,000			
42*					
0					
12.5		60,000			
42*					
0			Isothermal at 375°C	40,000	
42					
100					
300					
500					
700					
900					
1100					
100					
300					
500					
700					
900					
1100					

*Experiment run with and without flow rate adjustment accounting for ash plug volume. See Section 5.1.4.1.

5.1.1 CO + HC + NO Oxidation

A complete simulation of diesel exhaust would incorporate all of the gas species discussed in *Section 1.1.3*, so to test the DPFs catalytic performance the core samples were exposed to an exhaust stream made up of CO, NO and HC, each at a concentration of 500 ppm, 10% O₂ by volume, and the remainder made up of N₂ flowing at 40,000 hr⁻¹. The chemical concentration of each species was measured downstream of the filter during a temperature ramp programmed to proceed at 20°C/min. The results of this test are shown Figure 5-1. The desired reactions that indicate proper catalytic function are: (1) the conversion of CO to CO₂, (2) the conversion of HC to CO₂ and H₂O, and (3) the conversion of NO to NO₂.

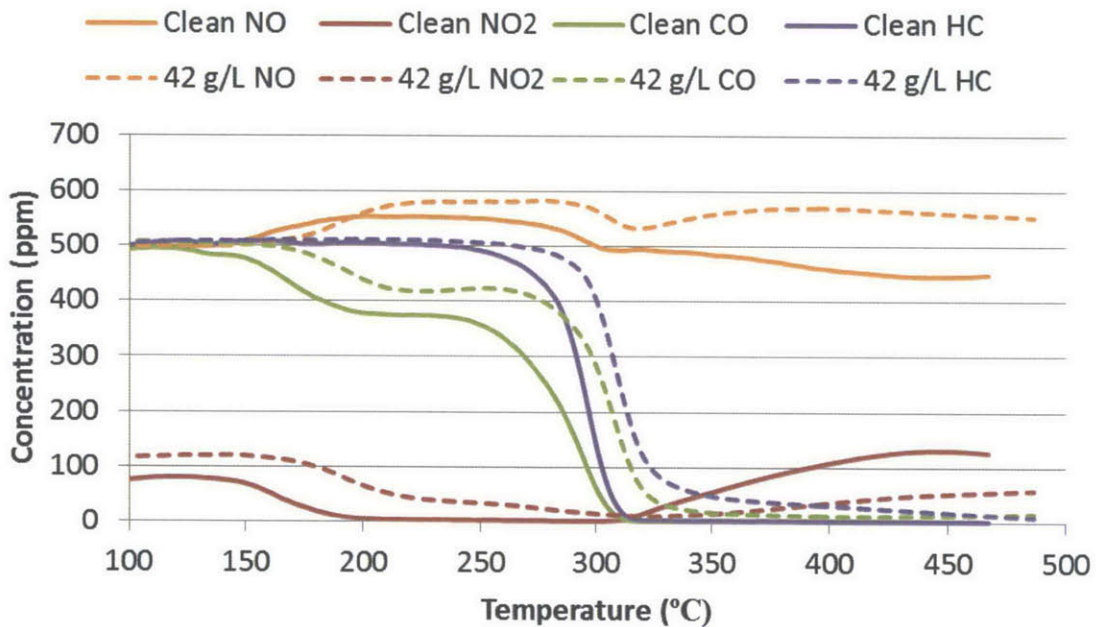


Figure 5-1 Simultaneous Conversion of CO, HC, and NO in a DPF

In examining only the clean or ash loaded DPF samples individually, it was obvious that a great deal of interaction occurred between the different chemical species as they competed for the catalyst surface area. At around 150°C the CO began to oxidize with the NO₂, but then reached a steady state once all of the NO₂ that existed in equilibrium with NO in the upstream compressed gas bottle was consumed. At a higher temperature, around 250°C, the remainder of the CO was oxidized, after which the HC oxidation was able to proceed. A peak in N₂O production was observed in both samples corresponding with the oxidation of HC. This indicates at least some of the propylene is reacting with NO_x as opposed to O₂. While the CO and HC were reacting there

was no NO_2 present in the downstream exhaust; this was because any NO_2 that may have been generated on the catalyst would immediately react with the CO or the HC, and be converted back to NO. Once the CO and HC were entirely consumed excess NO_2 was generated. The NO_2 concentration increased until it peaked around 450°C . Above this temperature the NO_2 was converted back to NO because NO is favored energetic at high temperatures. This type of behavior has been predicted by a thermodynamic model which shows once a certain threshold temperature is reached all NO_2 will be converted to NO as depicted in Figure 5-2.⁴³

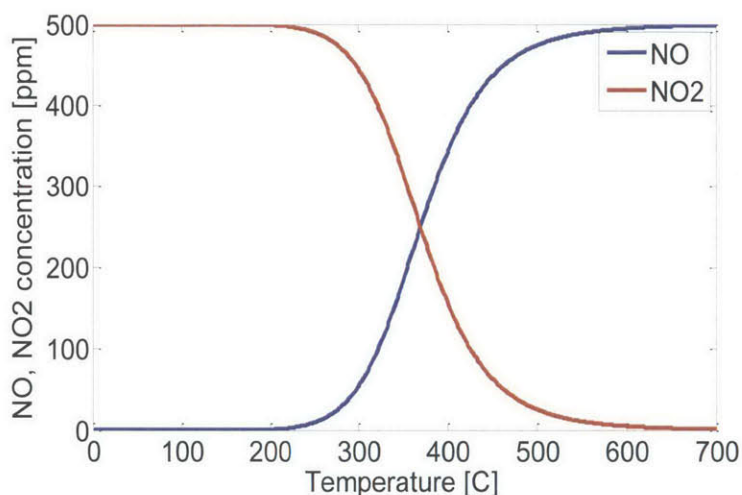


Figure 5-2 NO/ NO_2 Thermodynamic Equilibrium as Calculated by a Thermodynamic Model⁴³

In addition to the interaction between the different chemical species there was also a noticeable disparity between the clean and the 42 g/L ash loaded samples. The light-off temperatures for both the CO and HC reactions were shifted upwards as a result of the ash. This indicated that the presence of ash increased the amount of energy necessary for these species to react. Also, the amount of NO_2 generated at high temperatures was significantly lower for the ash loaded sample. This is particularly important because NO_2 is utilized in the combustion of soot, the primary purpose of a catalyzed DPF.

The competition between reactants leads to complex interactions on the catalyst surface that make it difficult to isolate all of the possible effects ash may have. In order to isolate the behavior of each reactant, each individual chemical species was considered on its own in an effort to understand the building blocks that made up the overall system of reactions. Particular emphasis was placed on examining the NO to NO_2 conversion capabilities of each filter.

5.1.2 CO and HC Conversion

In order to simplify the catalytic interactions, the oxidation of CO and HC were observed in isolation from all other oxidizing species. Each experiment was conducted under the same conditions as those of *Section 5.1.1*; namely, a flow rate of $40,000 \text{ hr}^{-1}$ and a stream consisting of 500 ppm of either CO or HC, 10% O_2 , and N_2 as the balance. The results of these tests are presented in Figure 5-3 and Figure 5-4.

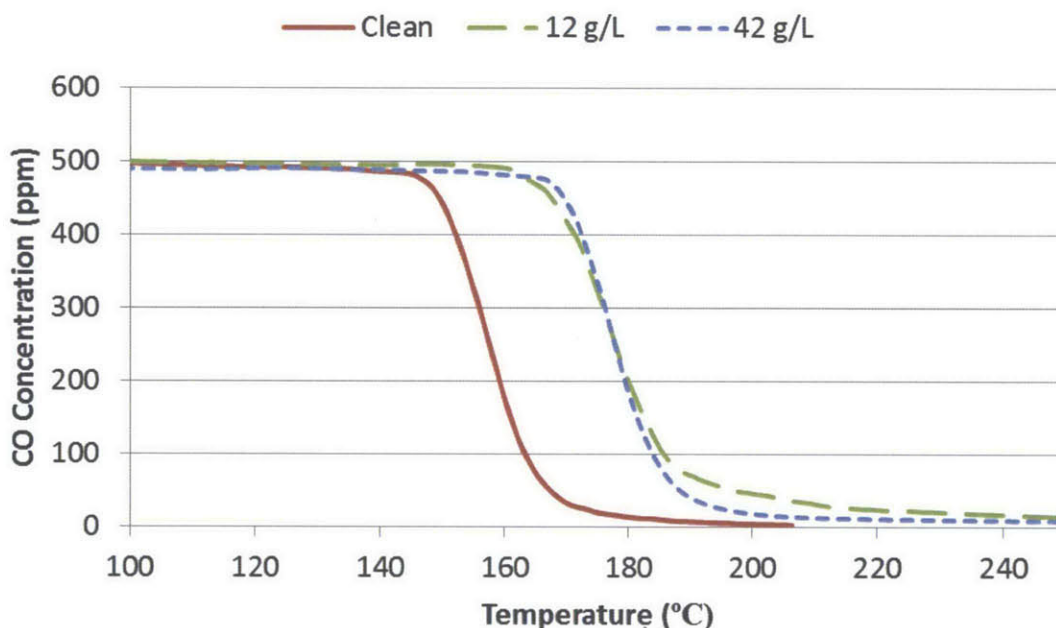


Figure 5-3 Ash Effect on CO Oxidation Light-off Temperature

As in the *Section 5.1.1*, the light-off temperature for CO oxidation was increased by about 20°C in the presence of ash. There was little difference between the 12.5 and 42 g/L ash loaded samples, suggesting the effect was the result of the initial deposition of ash, as opposed to the buildup of an ash plug or the increase in the thickness of the wall layer.

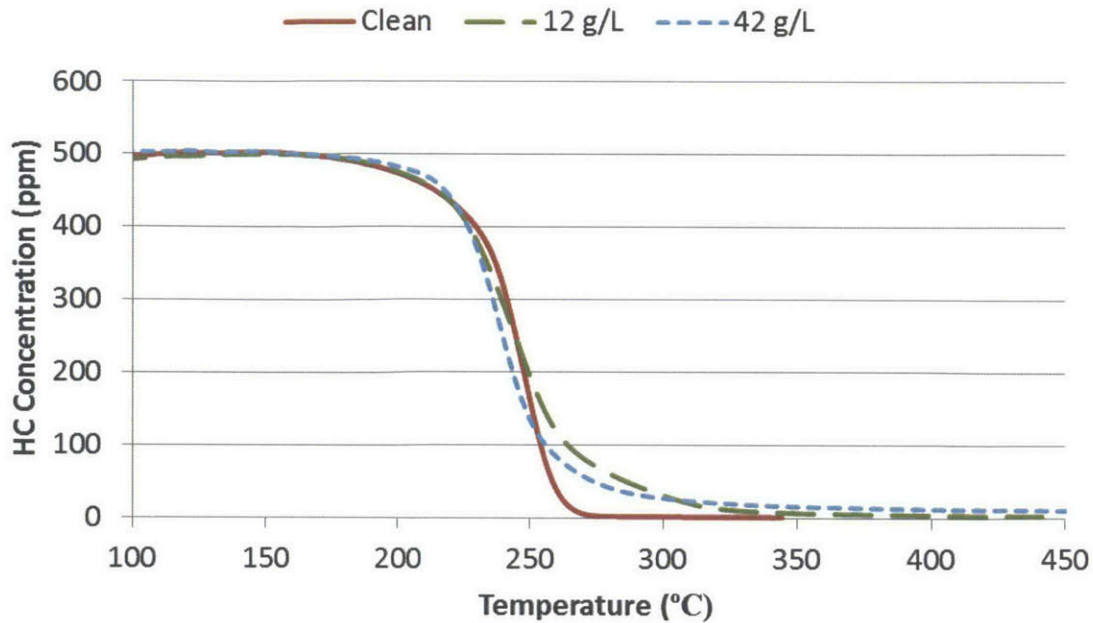


Figure 5-4 Ash Effect on HC Oxidation Light-off Temperature

There was, however, no impact on the light-off temperature for the oxidation of HC as a result of ash accumulation. This suggests there was still ample catalyst availability to initiate the HC conversion. Although the light-off temperature was not altered, the conversion was less complete, as evidenced by the change in slope between the clean and ash loaded samples in Figure 5-4. This may be attributed to increased pore diffusion resistance resulting from thermal aging³⁷ or it may have to do with HC adsorbing on the surface of the ash itself and then slowly releasing at slightly elevated temperatures. The adsorption hypothesis could be tested by using diffuse reflectance infrared Fourier transform spectroscopy (DRIFTS), which is capable of directly observing chemical species that are adsorbed on a surface.

Both results point to a decrease in catalytic activity which could negatively impact a filter's ability to oxidize soot. If the energy required to initiate a reaction increases, as was seen during CO oxidation, there would be an additional fuel penalty to the engine since more work would need to be expended in order to regenerate the soot. The result would be the same if the surface of the ash is adsorbing additional gaseous species necessitating additional energy to be expended in order to desorb the same species.

5.1.3 Desorption

This test was designed to investigate the adsorption and desorption characteristics of the clean and ash loaded DPF samples. Using the flow bench reactor, the samples each underwent a ramp in temperature at a rate of 20°C/min up to 600°C with 500 ppm of NO, HC, and CO, 10% O₂, and the remainder N₂ at a flow rate of 40,000 hr⁻¹. They were held above 600°C for 10 minutes and then cooled to below 50°C, all while still in the presence of the full mixture of gases. This procedure is necessary in order to ensure the required energy had been met for each gaseous species to desorb from the surface as it heats up and adsorb on the surface as it cools down. This facilitates a consistent initial state for each filter. The flow of each of the oxidizing species was then stopped and the sample was heated at a rate of 10°C/min back to over 600°C in the presence of only N₂.

Figure 5-5 depicts the concentration of each chemical species during the second increase in temperature in which the gases could only have been output through desorption. The gaseous species shown on this plot are the only ones that were detected by the FTIR. The data presented in this figure represents only the fraction of the test that occurred over the linear temperature ramp. Once the sample reached over 600°C it was maintained at that temperature until the concentration of each gaseous species was reduced to zero.

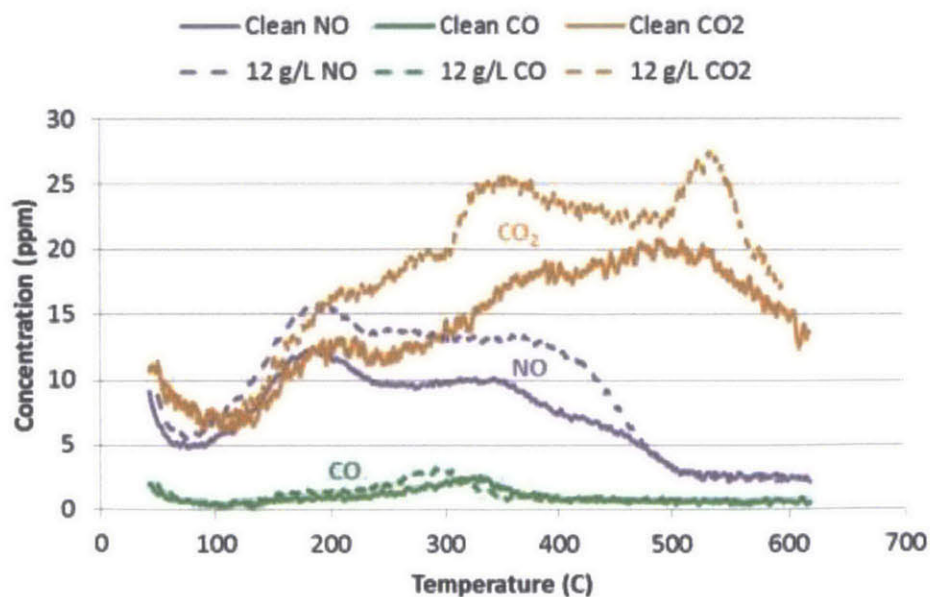


Figure 5-5 Gaseous Emissions from Clean and 12.5 g/L Ash Loaded DPF Desorbed from Surface during Temperature Ramp

There are two observations worthy of particular note in Figure 5-5: first, the molecules were still being desorbed from the surface up to 600°C (this result was the major motivation for the heated pre-treatment that was carried out before every other experiment so as to clear the surface of any adsorbed species); second, the magnitudes of these emissions were fairly low, on the order of 20 ppm, significantly less than 500 ppm, the standard concentration used as the input in the experiments conducted during this study.

The primary species desorbed from the surface were NO and CO₂. The CO₂ was not introduced to the system as CO₂, but results from the combustion of both CO and HC. The different peaks in this plot probably represent the desorption of these two different species. Since it was seen in Figure 5-1 that CO oxidized before HC, it is most likely that the initial peak is the result of the CO and the second peak the HC.

Integrating these curves over their entire duration – not only during the temperature ramps – gives a measure of the total emissions from the sample and therefore the amount of each species that was once adsorbed on the surface. In this way it was calculated that the ash loaded sample released 26% more emissions on a molar basis. This increase can be attributed to the additional adsorption capacity resulting from the surface area of the ash.

5.1.4 NO Oxidation

NO oxidation was of primary concern because of the NO₂ mechanism for the oxidation of soot. Several tests were run varying ash load, flow rate, and inlet NO concentration to understand the extent to which ash impacts NO₂ generation.

Most of the following plots are expressed in terms of NO destruction. Since the total amount of NO_x must be conserved, the amount of NO destroyed must be equal to the amount of NO₂ generated, and thus these two terms can be considered synonymous. The values expressed in this section were computed as the concentration of NO₂ output from the filter minus the NO₂ input into the filter all divided by the NO input into the filter.

5.1.4.1 Temperature Ramp

Each of the following temperature ramp experiments were conducted using 500 ppm of NO, 10% O₂, and N₂ as the balance. The temperature was increased at a rate of 10°C/min in order to

increase the level of consistency and resolution. The incoming NO_x was almost entirely NO, although some NO₂ was present in equilibrium with the NO in the compressed gas bottle.

Figure 5-6 depicts the NO destruction in a clean sample at different flow rates. The NO destruction was reduced as the velocity of the exhaust stream was increased because the chemical species had a shorter residence time inside the filter with which to react with the catalysts. Alternatively, it is possible that the catalyst particles became saturated with NO_x at the higher flow rates since each particle would theoretically be exposed to more NO_x molecules per unit time. The reduction in NO destruction did not follow a linear pattern in relation to the increase in flow velocity, but there was a clear trend.

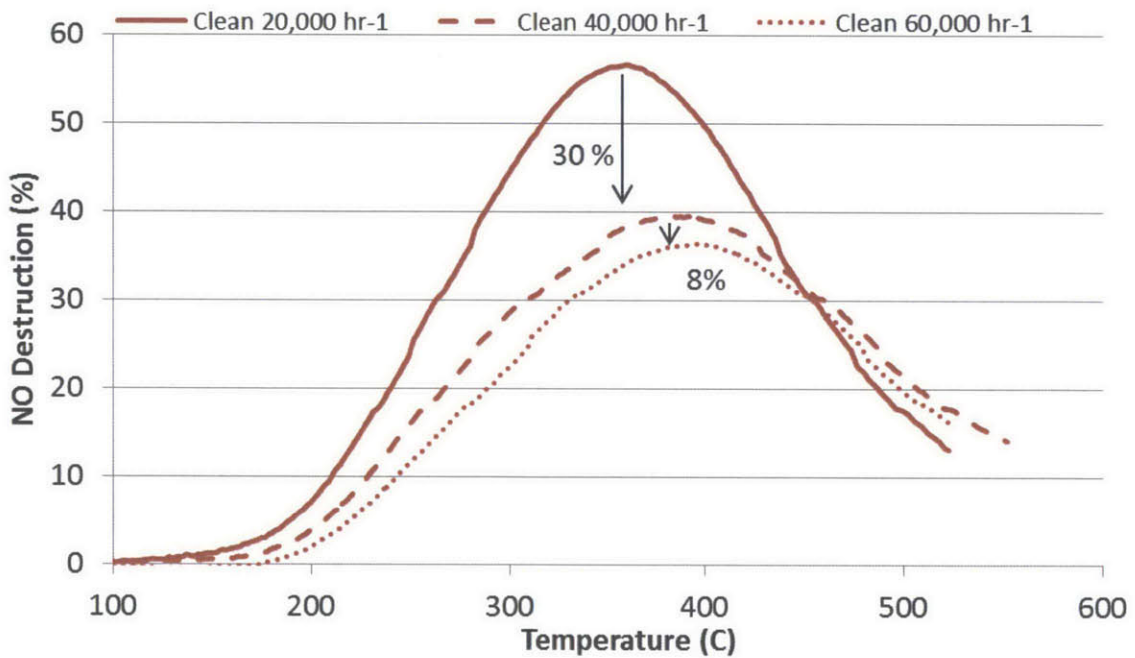


Figure 5-6 NO Oxidation in Clean DPF: Flow Velocity Dependence

The impact of ash on NO destruction at varying flow rates is depicted in Figure 5-7, Figure 5-8, and Figure 5-9. At each velocity there was a clear reduction in NO destruction with increasing ash load.

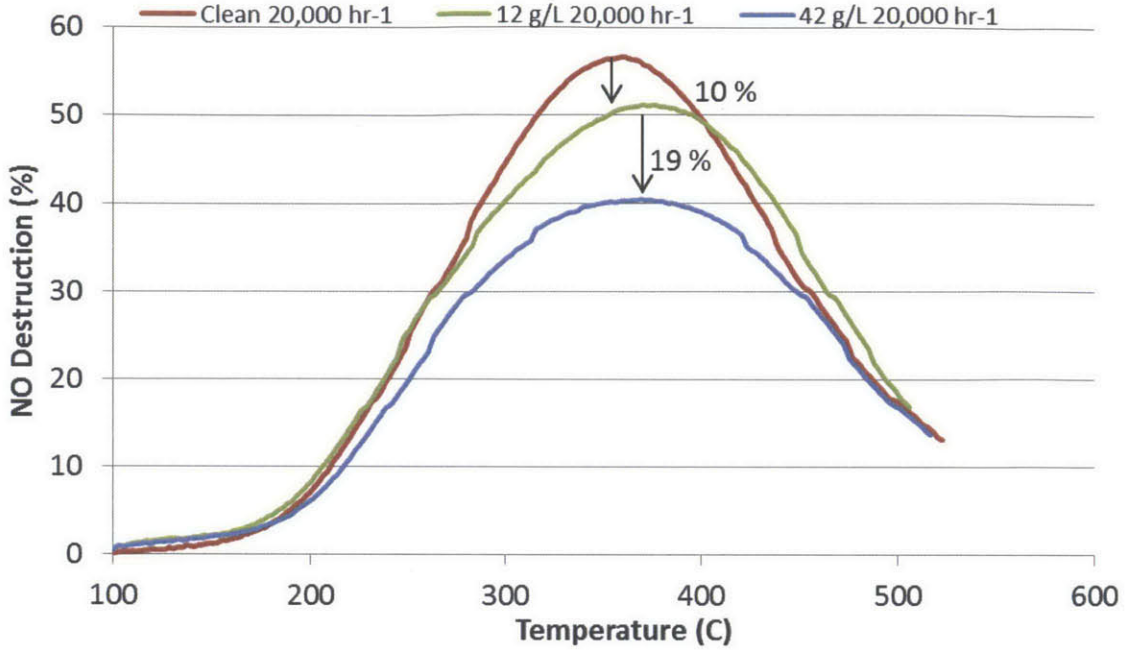


Figure 5-7 Ash Effect on NO Oxidation at 20,000 hr⁻¹

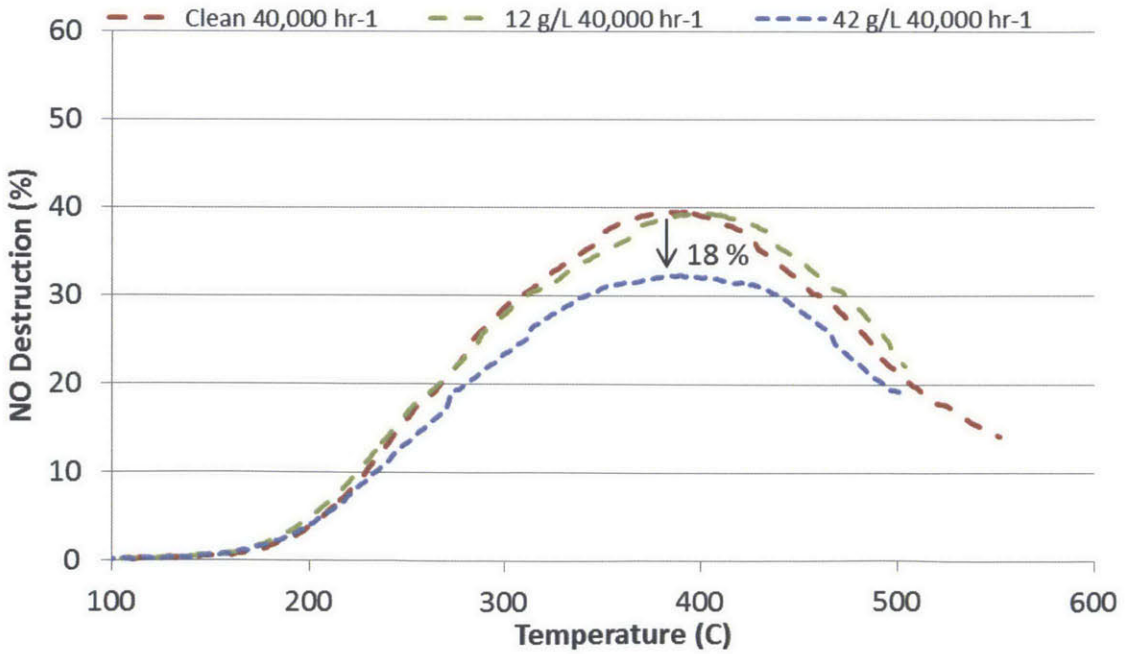


Figure 5-8 Ash Effect on NO Oxidation at 40,000 hr⁻¹

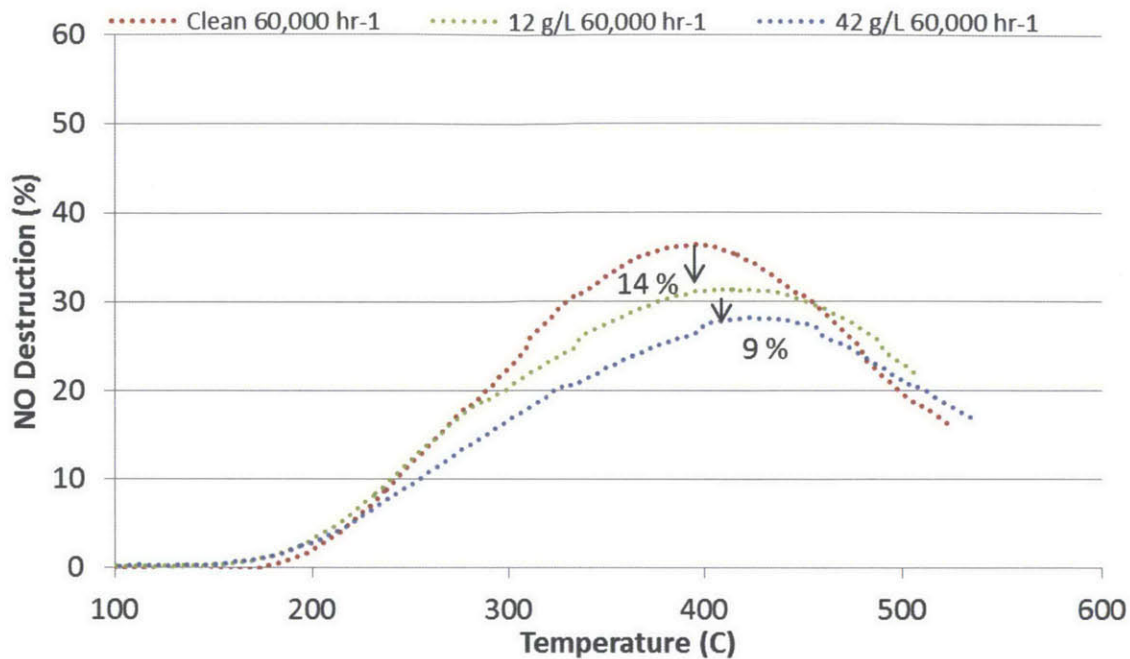


Figure 5-9 Ash Effect on NO Oxidation at 60,000 hr⁻¹

These results indicate that the NO destruction capabilities of the filter were reduced roughly 20-30% when fully ash loaded (42 g/L).

The peak NO destruction at each flow rate and for each sample is summarized in Figure 5-10. This figure clearly illustrates that there is a reduction in the NO destruction capability of a DPF as the result of both increased flow velocity and ash load. The 40,000 hr⁻¹ clean sample appears to be uncharacteristically low, but the result was duplicated during multiple repetitions of the same experiment.

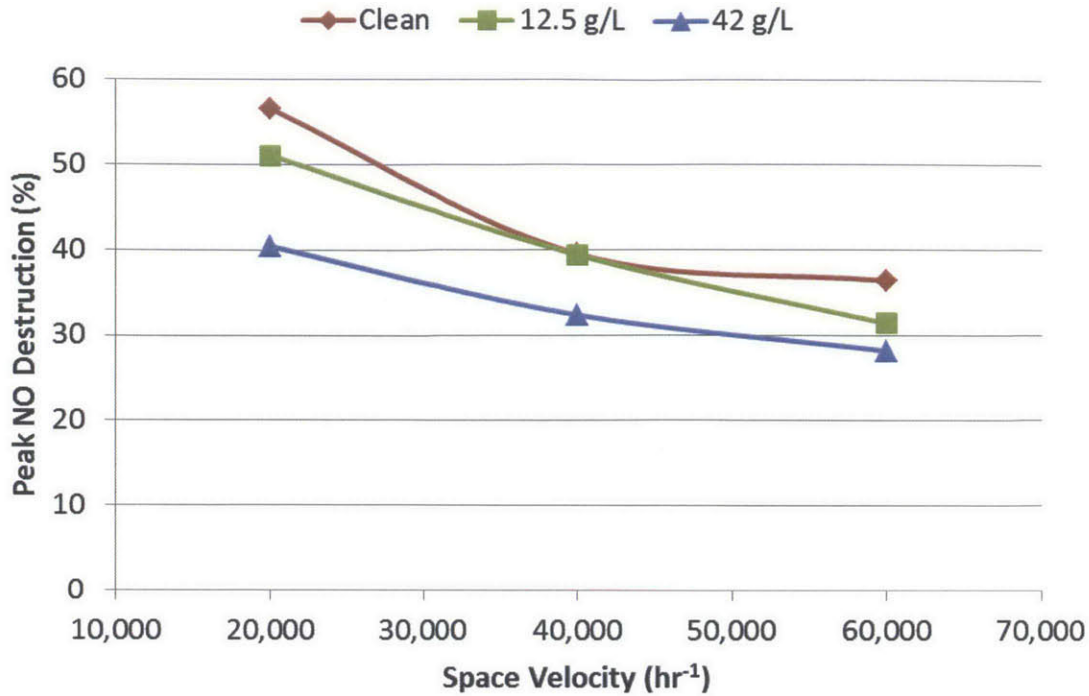


Figure 5-10 Peak NO Destruction for Clean and Ash Loaded Samples at Various Flow Velocities

As described in *Section 3.5*, the ash plug will increase the apparent flow velocity through the DPF by reducing its usable volume. In order to isolate this effect, the volumetric flow rate through the filter was reduced in the 42 g/L ash loaded sample in order to maintain the same space velocity such that only the volume of the DPF not filled with the ash plug was considered.

The average ash plug was found to be 31% of the total DPF length using X-Ray CT images taken by Dr. Carl Justin Kamp, a post-doctoral researcher in the Sloan Automotive Laboratory at MIT. These images, which are shown in Figure 5-11, each represent an internal slice of the DPF core sample. The ash plug can be clearly seen, as highlighted by the dotted yellow line. The same flow velocity reduction procedure was not performed for the 12.5 g/L ash loaded sample since it has a much shorter ash plug length as seen in Figure 5-12.

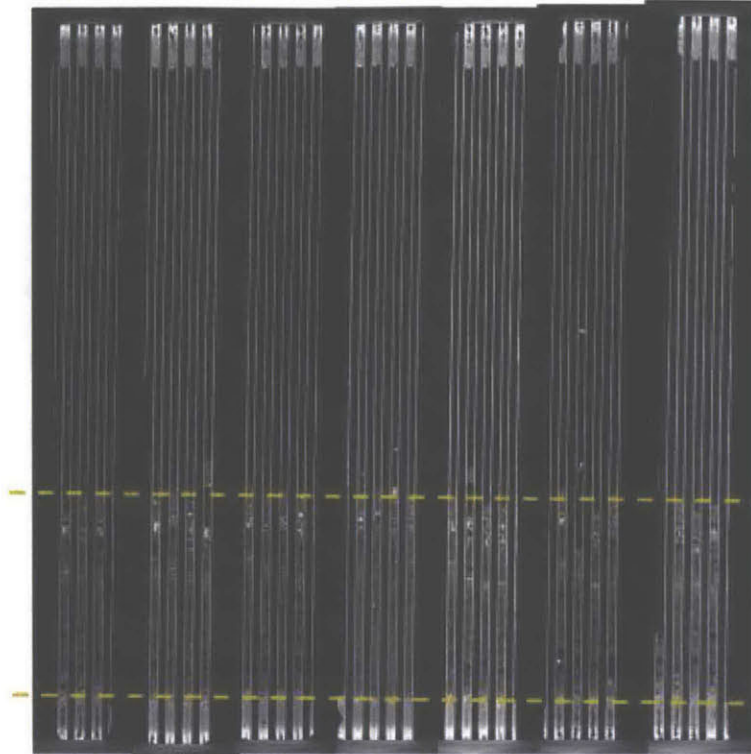


Figure 5-11 X-Ray CT Scans from 42 g/L Ash Loaded DPF Core Sample

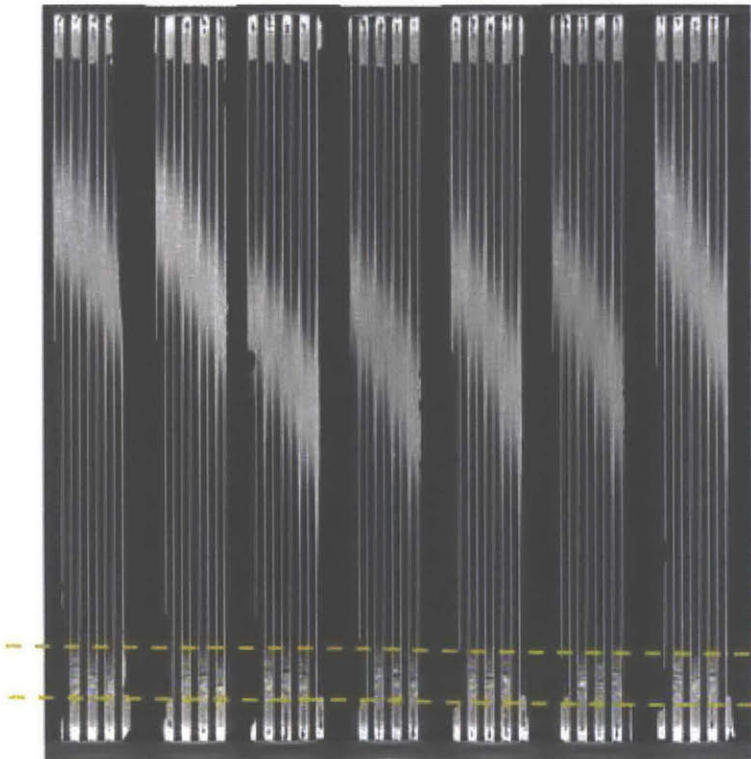


Figure 5-12 X-Ray CT Scan of 12.5 g/L Ash Loaded DPF Core Sample

Knowing the ash plug length of the 42 g/L ash loaded sample was 31% of the total filter length, the volumetric flow was reduced by 69%. This resulted in flow the filter at an adjusted space velocity of 40,000 or 60,000 hr⁻¹, consistent with the space velocity through the clean sample. The test was not conducted at 20,000 hr⁻¹ because it was feared the low flow rate would not generate enough convective cooling power to safely operate the heater. The results are shown in Figure 5-13 and Figure 5-14.

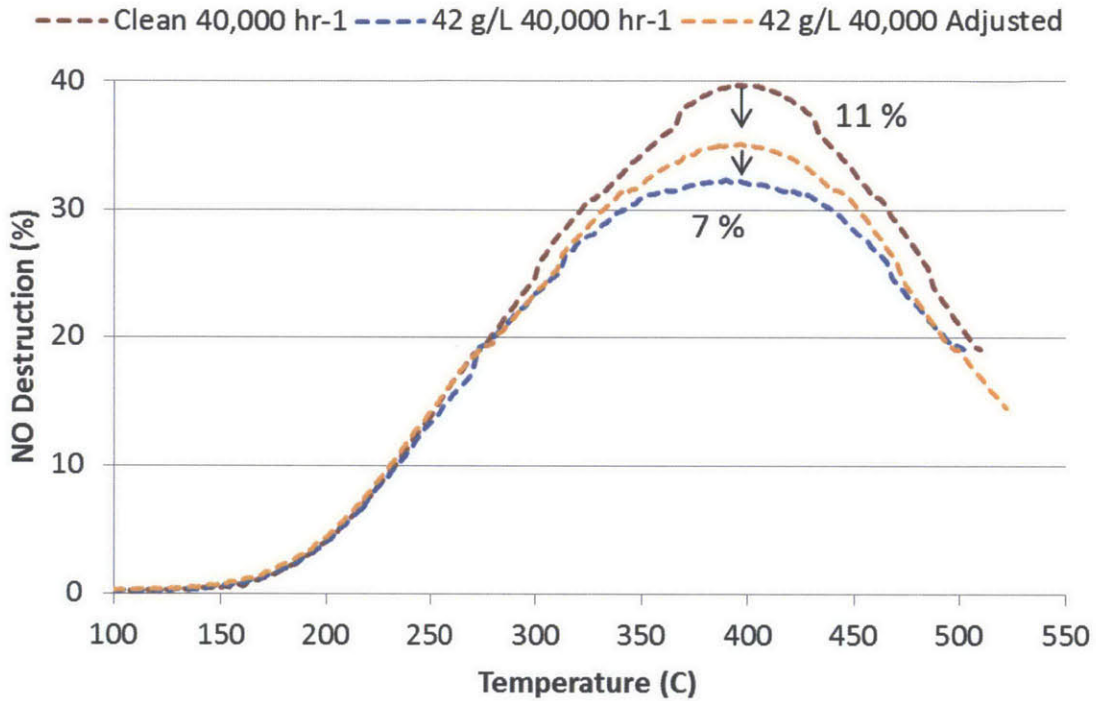


Figure 5-13 NO Oxidation at 40,000 hr⁻¹: Velocity Adjusted for Ash Plug Volume

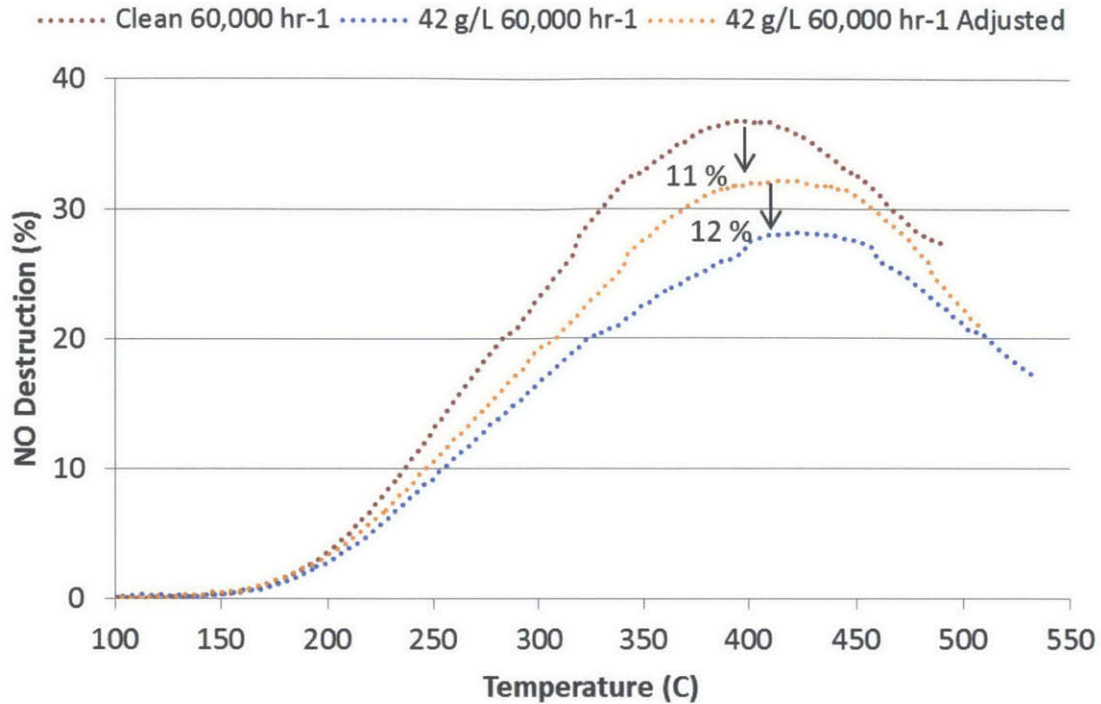


Figure 5-14 NO Oxidation at 60,000 hr⁻¹: Velocity Adjusted for Ash Plug Volume

Figure 5-13 and Figure 5-14 indicate that while the adjusted flow rate did improve the NO destruction capabilities of the ash loaded sample, it did not return to the same level of performance as the clean filter. This suggests that both the ash plug and the wall layer contribute to the reduced catalytic activity of the filter. Each mode of ash deposition contributed fairly equally – on the order of 10% – to the loss in NO destruction.

5.1.4.2 Isothermal NO_x Step Experiment

In addition to the temperature ramp experiments discussed above, an isothermal test was conducted to examine whether the NO conversion efficiency changes with the concentration of NO entering the DPF. The results in this section were all taken at 375°C, which is near the point of peak NO destruction observed in *Section 5.1.4.1*. The NO input was increased from 100 ppm to 1100 ppm in increments of roughly 200 ppm. At each step a steady state was established. The results of this test for both a clean and 42 g/L ash loaded DPF are presented in Figure 5-15, Figure 5-16, and Figure 5-17 .

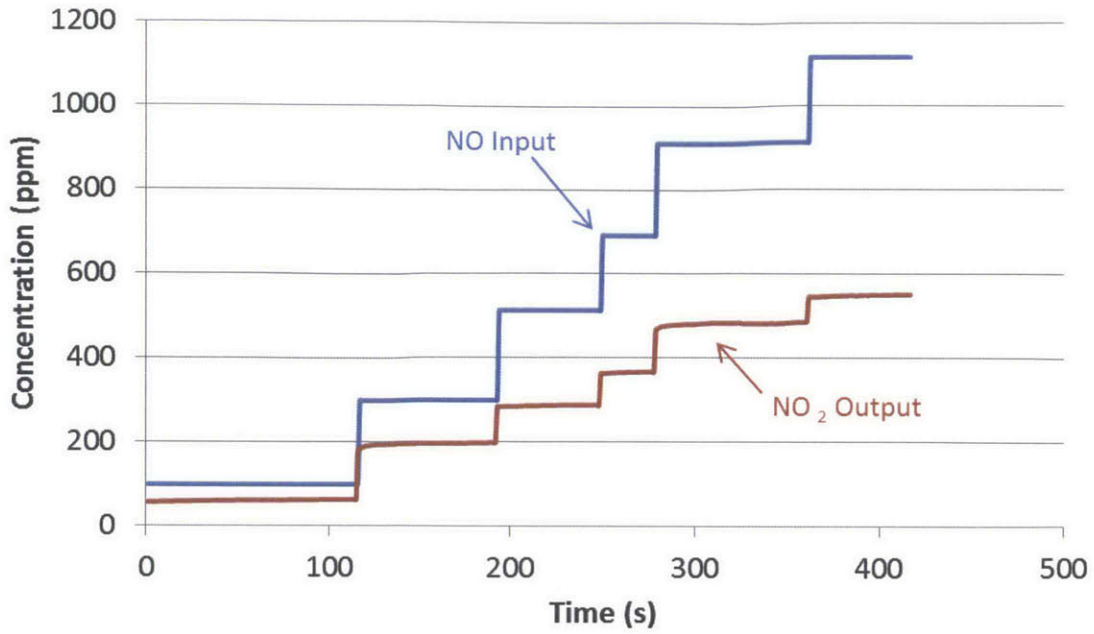


Figure 5-15 Clean DPF Isothermal NO Oxidation

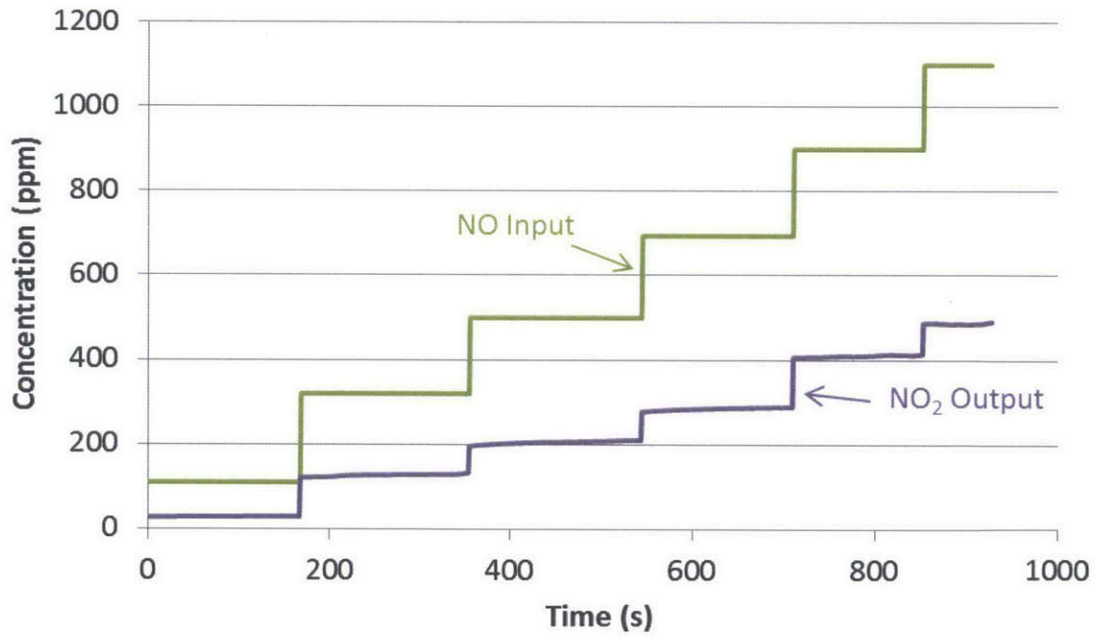


Figure 5-16 42 g/L Ash Loaded DPF Isothermal NO Oxidation

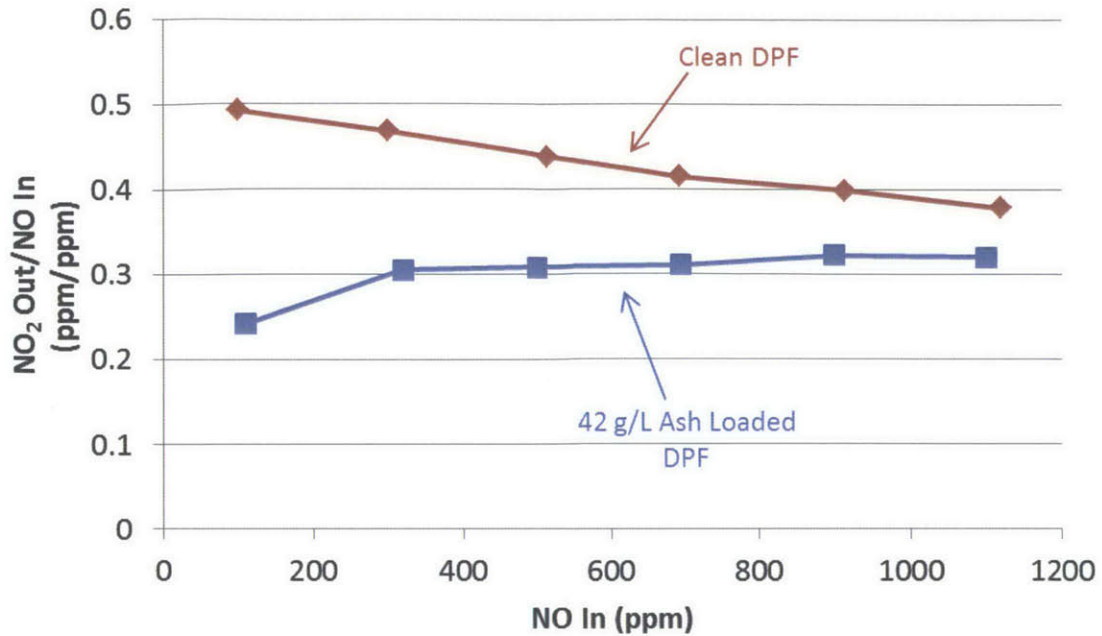


Figure 5-17 Isothermal NO to NO₂ Conversion with increasing NO Concentration

There was a clear loss in NO destruction efficiency for the ash loaded sample at each concentration increment. The loss in NO_x conversion measured at an inlet NO concentration near 500 ppm was consistent with the NO destruction value measured during the temperature ramp experiment in *Section 5.1.4.1*.

It was expected that increasing the NO input would result in a decrease in the conversion efficiency of the DPF because the surface area of the catalyst is finite. As the concentration of NO increases a smaller fraction of it should be able to adsorb onto the catalyst surface area and react. The overall magnitude of NO₂ generated should increase but, not the conversion efficiency. This was the behaviour exhibited by the clean sample; however, the ash loaded DPF behaved differently in that the NO conversion efficiency increased with the NO input. One possible explanation is that this occurred because at low concentrations a higher percentage of the NO_x could adsorb onto the ash surface. This hypothesis is supported by the results presented in *Section 5.1.3* in which NO adsorption/desorption was observed to occur around this temperature. If the ash surface became saturated with NO_x at a certain point, it would serve to hinder the conversion performance at the lower concentrations more than at higher concentrations, which could result in the observed behaviour.

5.2 Soot Oxidation

In *Section 5.1* it was shown that ash has a negative impact on the ability of DPF catalysts to generate NO_2 . The following results will examine the impact of this loss in catalytic activity on the oxidation of soot. As discussed in *Section 3*, a reduction in soot oxidation performance would result in a direct fuel penalty if the aftertreatment system was relying on passive regeneration.

Two primary experiments were conducted: (1) the oxidation of soot over a temperature ramp, and (2) the isothermal oxidation of soot in the passive regime. In both cases the samples underwent a pre-treatment step in which they were heated in pure nitrogen to remove any volatile substances adsorbed in the filter and oxidize the bulk of the SOF in the PM, leaving only carbon soot. Unlike the pre-treatment procedure used during the gaseous conversion experiments, the temperature was only increased to 350°C in order to avoid the possible formation of graphite, a development that was unlikely to occur on an actual vehicle and one that would irreversibly alter the soot in a way that made oxidation nearly impossible.

5.2.1 Temperature Ramp

The soot oxidation experiments conducted over a temperature ramp utilized simulated exhaust at a space velocity of $40,000 \text{ hr}^{-1}$, consisting of 500 ppm NO, 10% O_2 , and the remainder N_2 . The temperature was increased at a rate of $10^\circ\text{C}/\text{min}$ from below 50°C to over 600°C . As soot oxidizes its main products are CO and CO_2 , which can be directly measured using the FTIR. Any CO that is produced will be immediately converted to CO_2 on the catalyst surface, so the concentration of CO_2 downstream of the filter represents all of the carbon that has been oxidized. The raw data for a soot oxidation experiment conducted on a clean DPF is shown in Figure 5-18.

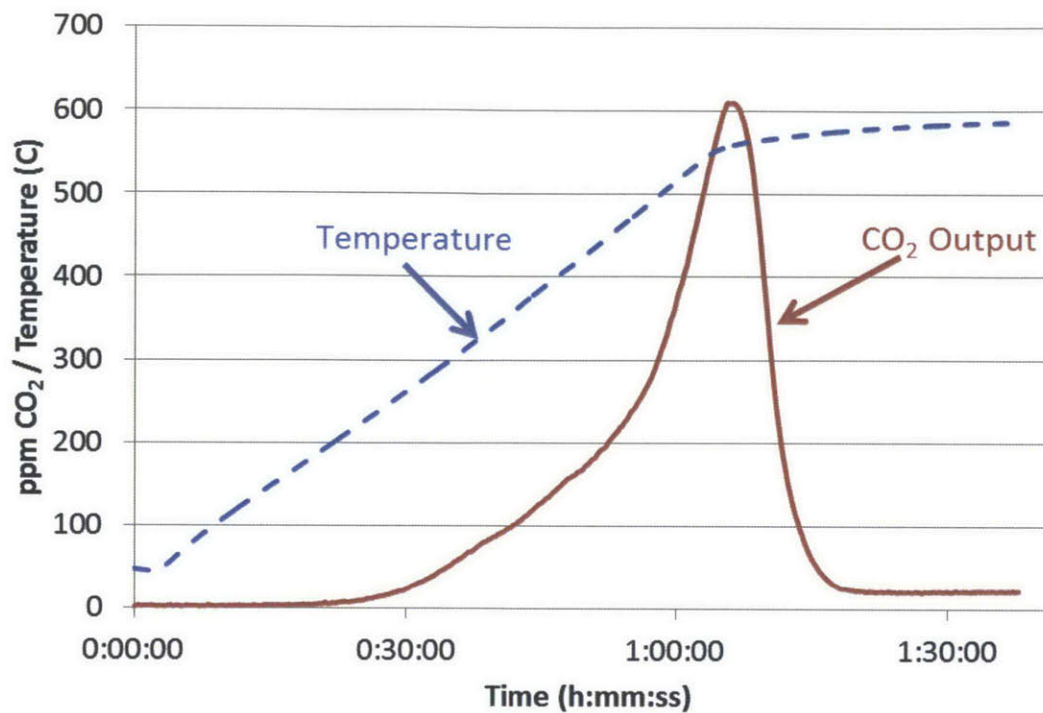


Figure 5-18 Direct Measurement of CO₂ output from Clean DPF during Regeneration

The ppm data was converted to a formation, or reaction, rate using a series of equations outlined below. The volumetric flow rate through the filter was related to the measured volumetric flow rate at the inlet of the system through the ideal gas law (Eq. 5-1); as was the number of moles held in the filter volume (Eq. 5-2).

Eq. 5-1

$$\dot{V} = \left(\frac{T}{T_{in}} \right) \dot{V}_{in}$$

Eq. 5-2

$$\frac{n_{total}}{V} = \frac{P}{\tilde{R}T}$$

The number of moles of CO₂ produced per second can be related to the molar fraction of the CO₂ present in the flow, the total number of moles per filter volume, and the volumetric flow rate through the filter (Eq. 5-3).

Eq. 5-3

$$\frac{mol_{CO_2}}{s} = \left(\frac{n_{CO_2}}{n_{total}} \right) \left(\frac{n_{total}}{V} \right) \dot{V}$$

Substituting Eq. 5-1 and Eq. 5-2 into Eq. 5-3, and recognizing that the molar fraction of CO₂ was directly measured as the ppm output of CO₂ (multiplied by 10⁻⁶), yields Eq. 5-4.

Eq. 5-4

$$\frac{mol_{CO_2}}{s} = (ppm_{CO_2} 10^{-6}) \left(\frac{P}{\bar{R}T_{in}} \right) \dot{V}_{in}$$

As described above, a soot oxidation reaction in a catalyzed DPF results almost exclusively in the production of CO₂. Therefore, it can be safely assumed that for every mole of carbon oxidized one mole of CO₂ was produced.

In order to calculate the formation rate, it was necessary to normalize the moles of carbon released/oxidized per second by the amount of carbon remaining on the DPF. The fraction of carbon left on the surface at any point in time was calculated by subtracting from 1 the integral of the moles of carbon produced per second from the onset of the experiment until the point in time under consideration (Eq. 5-5), and dividing by the integral of the carbon released per second over the entire experiment (Eq. 5-6).

Eq. 5-5

$$mol_C \text{ oxidized} = \int_{t_i}^t \left(\frac{mol_C}{s} \right) dt$$

Eq. 5-6

$$fraction \text{ left} = X_C = 1 - \frac{\int_{t_i}^t \left(\frac{mol_C}{s} \right) dt}{\int_{t_i}^{t_f} \left(\frac{mol_C}{s} \right) dt}$$

Multiplying by the molecular weight of carbon and dividing by the initial mass of soot deposited on the filter yields the formation rate of carbon oxidation (Eq. 5-7).

Eq. 5-7

$$Formation \text{ rate} = k = \frac{\left(\frac{mol_C}{s} \right) (MW_C)}{m_{c,i}(X_C)} \left[\frac{mmol_C \text{ released}}{mol_C \text{ available} * s} \right]$$

The data presented in Figure 5-18 has been converted to formation rate in Figure 5-19. The units, as shown in Eq. 5-7, are mmol of carbon released per second per mol of carbon available for oxidation.

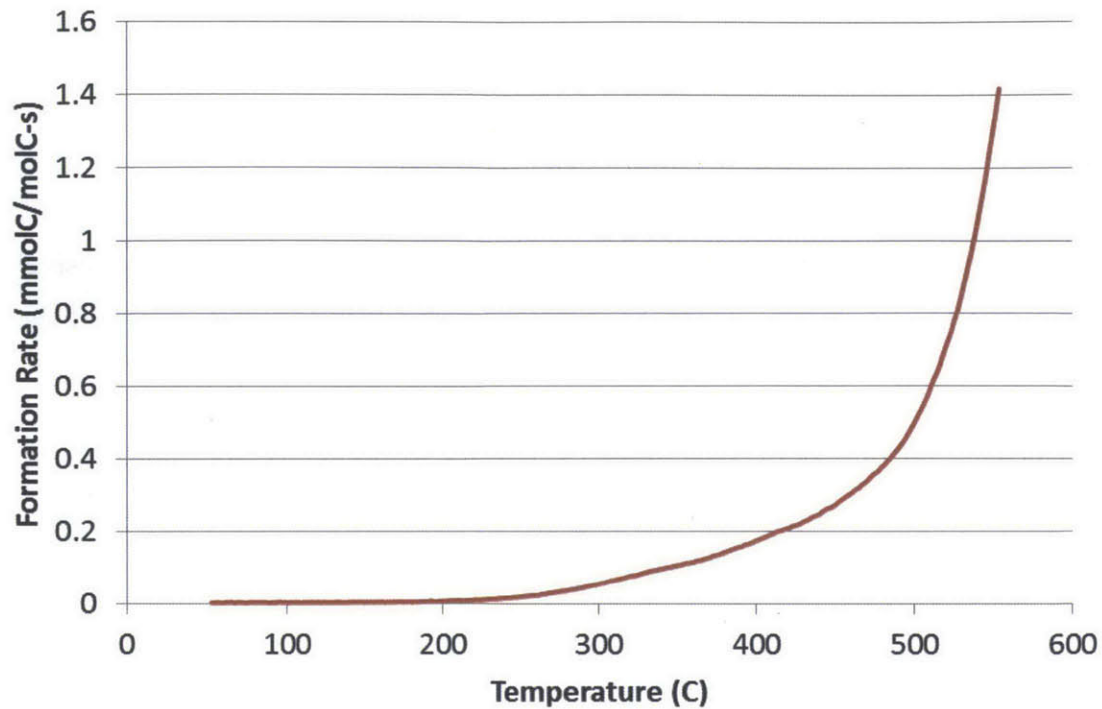


Figure 5-19 Plot of Formation Rate vs. Temperature for a Clean DPF during Regeneration

The formation rate can be described by the Arrhenius Equation discussed in Section 3.1. Taking the natural logarithm of Eq. 3-1 yields Eq. 5-8, which is in the linear form $y = mx + b$ where $y = \ln(k)$, $m = \frac{E_a}{R}$, $x = \frac{1}{T}$, and $b = \ln(A)$. Thus, if the natural logarithm of the formation rate is plotted against the inverse of the temperature, any linear regions represent different chemical reaction mechanisms. Graphs of this type are called Arrhenius Plots, and they can be used to extract the activation energies and pre-exponential factors of chemical reactions. The Arrhenius Plot for a soot oxidation experiment over the entire range of temperature used in these experiments is shown in Figure 5-20.

Eq. 5-8

$$\ln(k) = \ln(A) - \frac{E_a}{R} \left(\frac{1}{T} \right)$$

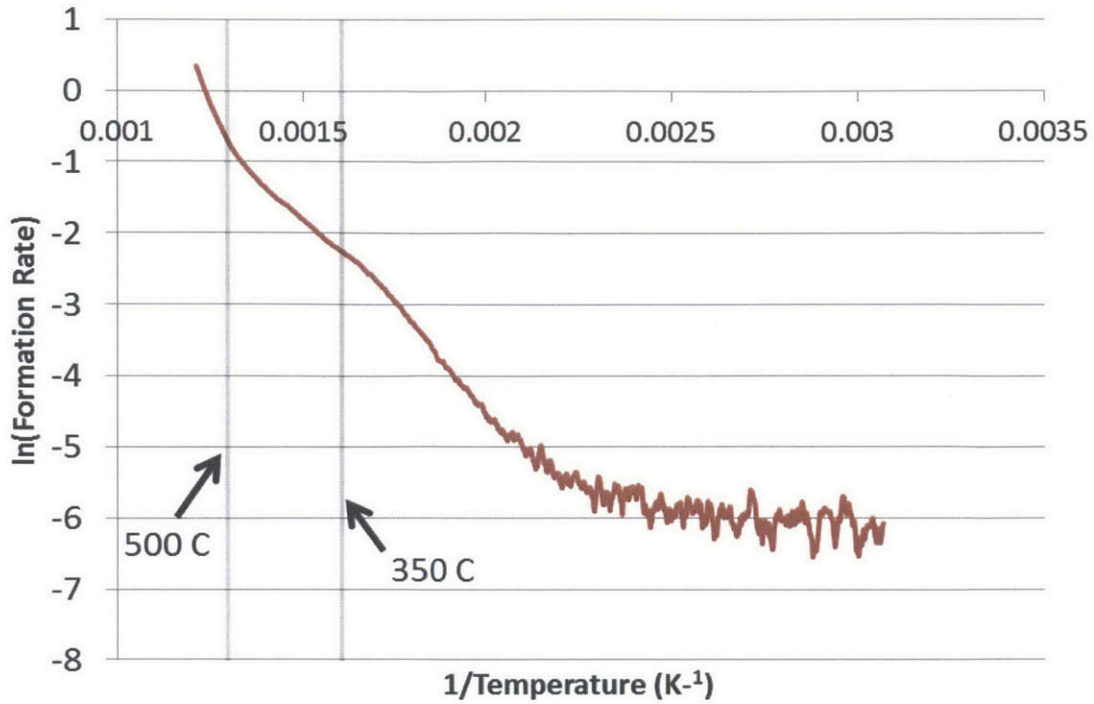


Figure 5-20 Arrhenius Plot: Soot Oxidation Reaction for Clean DPF

Active and passive soot oxidation are both represented in distinct regions of Figure 5-20. Active regeneration was observed at temperatures greater than approximately 525°C, indicated by the steep linear portion of the curve closest to the origin. Passive regeneration occurred at lower temperatures, between roughly 325-425°C as indicated by the linear slope in the middle of the chart. The portions of the Arrhenius Plot representing active and passive regeneration have been isolated in Figure 5-21 and Figure 5-22 respectively, which depict the curves generated by both a clean and 42 g/L ash loaded DPF core sample.

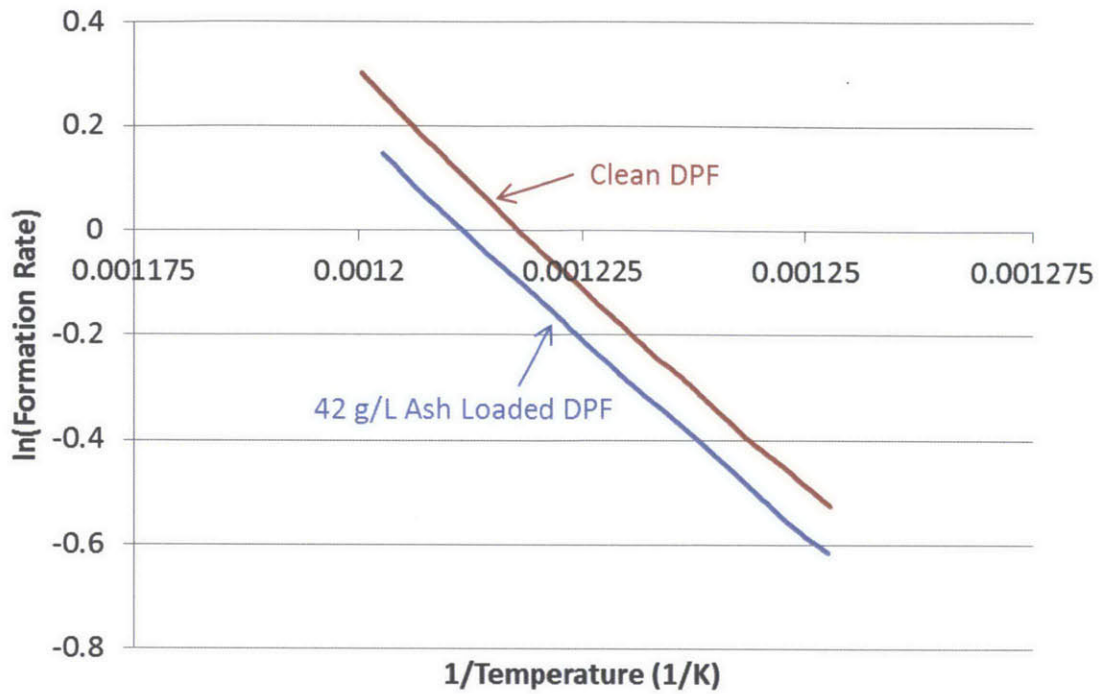


Figure 5-21 Arrhenius Plot of Soot Oxidation Reaction: Active Oxygen Mechanism (>525°C) for Clean and 42 g/L Ash Loaded DPFs

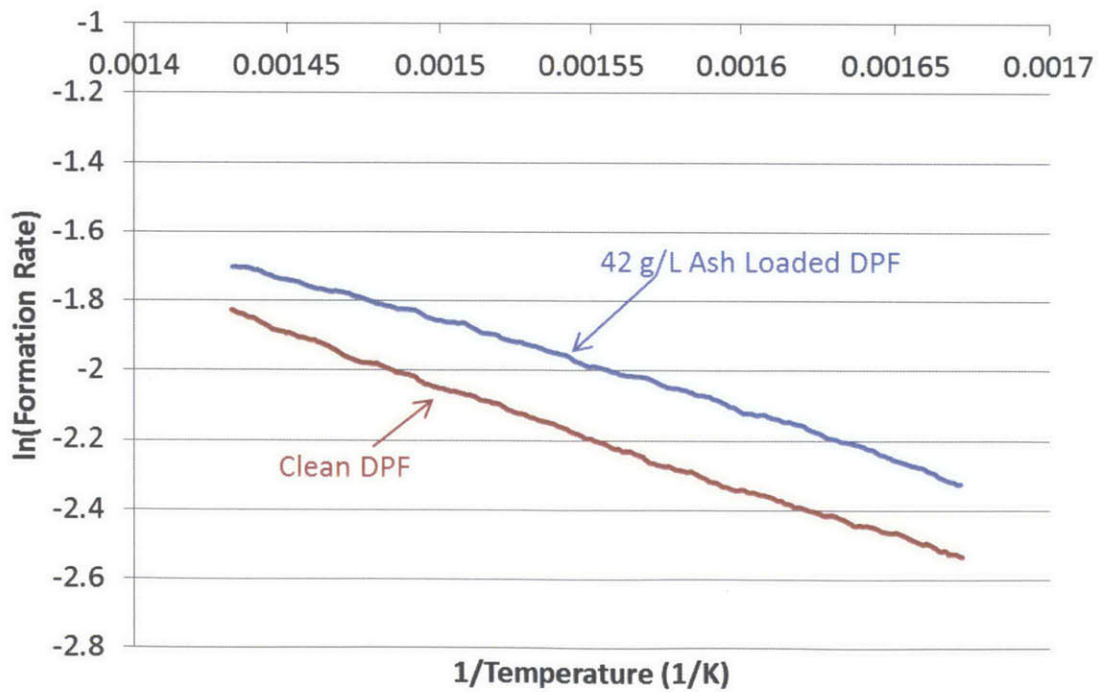


Figure 5-22 Arrhenius Plot of Soot Oxidation Reaction: Passive NO₂ Mechanism (325-425°C) for Clean and 42 g/L Ash Loaded DPF

Within each temperature region there was little change in slope between the clean and ash loaded DPF samples. The activation energies in the high temperature range, representative of active regeneration, were calculated to be 123 and 124 kJ/mol for the clean and ash loaded filters respectively. In the lower temperature passive regeneration regime, the activation energies were found to be 24 and 20 kJ/mol for the clean and ash loaded filters respectively. These values are all similar to those reported in literature.^{39,40,41} The small reduction in activation energy experienced by the ash loaded sample suggests the ash may function as a slight catalyst and promote the oxidation of soot. However, the reduction in activation energy is within the degree of experimental error, so it would be premature to draw too strong a conclusion. The consistency of the activation energy measurements indicate that the chemical mechanism through which passive soot oxidation is occurring is not altered by the presence of ash.

Figure 5-21 and Figure 5-22 also reveal a shift in the y axis, indicative of a change in pre-exponential factor. However, unlike the slope, which was found to be consistent during repeated experiments, the vertical shift of the plots varied significantly across different trials of the same test. Examples of this variation can be seen in the Appendix (Figures A.1 and A.2). The pre-exponential factor is incredibly sensitive to a number of factors related to the experimental set-up. It is believed that this variation may be due to inconsistencies in the trench exhaust system, which induced a negative pressure on the outlet of the DPF which changed depending on which other apparatuses were operating in the laboratory at a given time. Additionally, the high thermal capacitance of the steel tubes that housed the DPF core samples may have introduced additional heat transfer to and from the DPF samples impacting the results. Switching from steel to quartz tubes would improve the thermal stability of the flow bench system.

5.2.2 Isothermal Soot Oxidation

The results from the temperature ramp experiments suggest that the accumulation of ash does not alter the activation energy of passive or active oxidation of soot. However, it provided little insight into the impact of ash on the pre-exponential factor.

DPF catalysts do not play a role in active soot regeneration, so to further investigate catalytic activity the low temperature oxidation regime was investigated using isothermal experiments. The clean and 42 g/L ash loaded DPF core samples were loaded with soot to 5.0 and 5.3 g/L respectively and oxidized in a simulated exhaust stream at a space velocity of 40,000 hr⁻¹

consisting of 500 ppm NO, 10% O₂, and the balance made up by N₂. During each test, the sample was maintained at 400°C for 1 hour, and the CO₂ produced was measured. The results of these experiments are shown in Figure 5-23 and Figure 5-24.

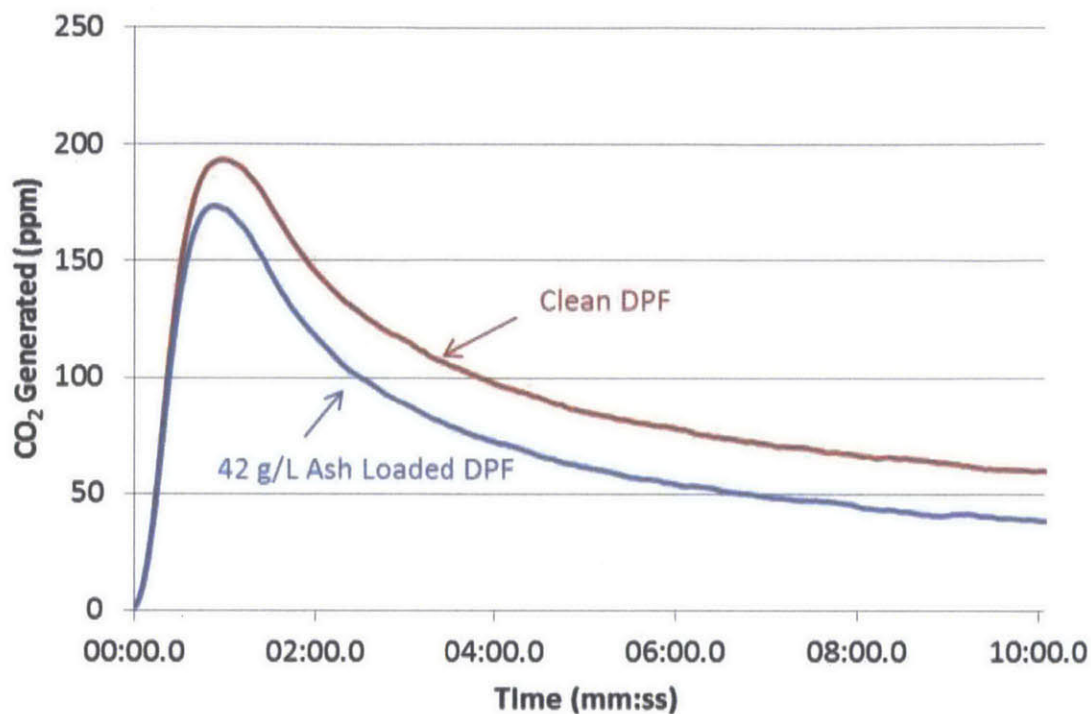


Figure 5-23 Isothermal Soot Oxidation Reaction of Clean and 42 g/L Ash Loaded DPFs (10 minutes)

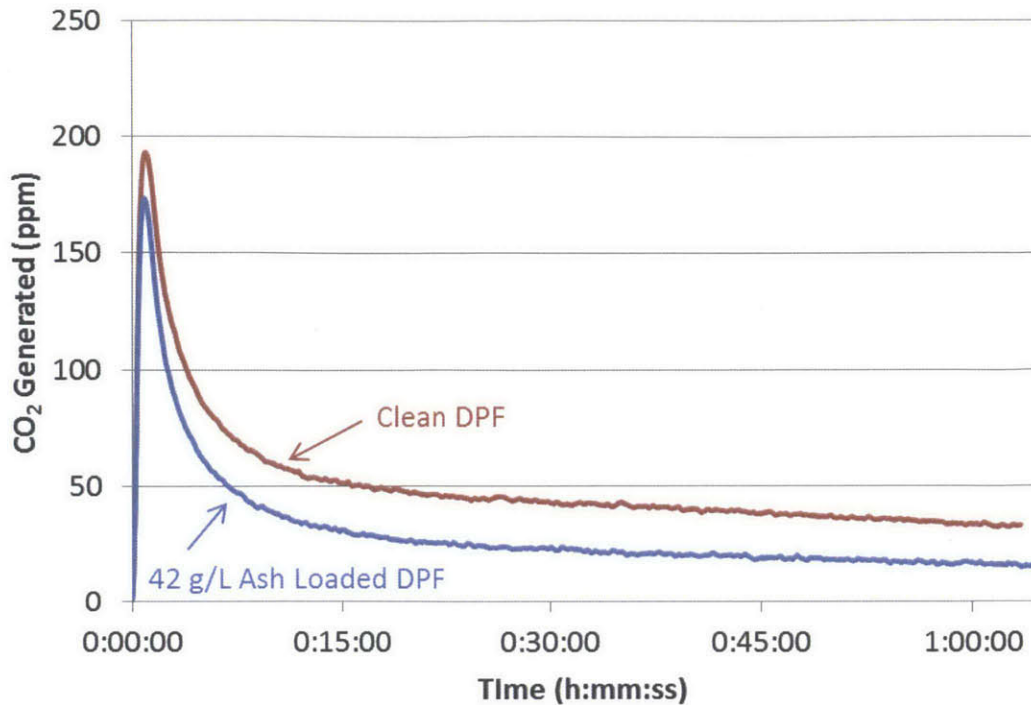


Figure 5-24 Isothermal Soot Oxidation Reaction of Clean and 42 g/L Ash Loaded DPFs (1 hour)

Despite the fact that the clean DPF is loaded with slightly more soot than the ash loaded filter, it consistently generated more CO₂, indicating the clean sample was oxidizing the soot faster than the ash loaded sample. The peak CO₂ production of the ash loaded DPF was roughly 10% lower than that of the clean sample.

Over the course of this experiment not all of the soot loaded onto the sample was oxidized; however, it can be reasonably assumed that the clean sample would have become free of soot faster than the ash loaded sample, since over the entire duration of the experiment it was releasing more CO₂ and thus oxidizing more soot. This result indicates that ash does in fact hinder the regeneration of soot in a DPF.

Since it has been shown that the ash does not impact the chemical reaction mechanism during regeneration, as evidenced by the lack of change in the activation energy, the pre-exponential factor must have been altered. This could result from the physical masking of catalyst particles, the thickness of the ash wall layer through which the NO₂ must back diffuse in order to reach the soot, the increased wall flow velocity resulting from the ash plug, or thermal aging. An experimental study of the four possible causes, noted above, that are involved in the alteration of

the pre-exponential factor, with an emphasis upon determining which of them dominates the system, would constitute a positive and useful extension of this study.

6 CONCLUSIONS

The objective of this study was to investigate the extent to which ash impacts DPF catalytic activity, which is vital for the passive regeneration of soot, the conversion of NO to NO₂, and the oxidation of CO and HC. Two laboratory aged DPF samples that were loaded to 12.5 and 42 g/L of ash, simulating 72,000 and 240,000 miles of operation respectively, were compared to a clean, previously unused filter in a number of experiments designed to compare the ability of each filter to promote gaseous chemical conversion and soot oxidation.

6.1 Summation of Results

Desorption experiments were used to determine that chemical species can remain adsorbed on the surface of a DPF up to 600°C. The addition of ash provides increased surface area, which was shown to increase the capacity for adsorption; however, it did not significantly shift the temperatures at which the species were desorbed. A DPF loaded with 42 g/L of ash was found to exhibit a 26 % increase in the number of moles that could be adsorbed on the filter.

It was found that the light-off temperature for CO conversion was increased by about 20°C when ash was present in the DPF. There was no measured difference between the two ash loaded samples, suggesting the effect was the result of the initial deposition of ash and not proportional to the amount accumulated. There was no shift in HC light-off temperature, but the oxidation was observed to occur more slowly, i.e., less completely, in both of the ash loaded DPFs compared to the clean sample. Both of these results indicate a loss in catalytic activity as a result of aging. Since the passive oxidation of soot relies on the activity of the catalyst, this reduction suggests the passive regeneration capabilities of a DPF may be negatively affected by ash.

The NO to NO₂ conversion capability of a DPF was shown to decrease significantly in the presence of ash. Depending on the space velocity of each test, the NO destruction efficiency was reduced by roughly 1-14 % when the sample was loaded with 12.5 g/L and 18-29% when it was loaded with 42 g/L of ash. This is an important finding because the catalyzed oxidation of soot in a DPF relies heavily on the production of NO₂. If a DPF's ability to promote the conversion of NO to NO₂ is reduced, there will likely be a negative impact on its ability to passively oxidize soot.

It was observed that the ability of a DPF to generate NO_2 was also reduced at increased flow velocities due to the shortened residence time of the molecules passing through the filter. The effect of the ash plug in a highly loaded sample (42 g/L) was isolated by reducing the volumetric flow rate such that the space velocity was calculated using only the section of the DPF not filled with the ash plug. Correcting the space velocity was shown to improve the performance of the ash loaded filter by roughly 10%, which accounted for roughly half of the total impact of the ash. This suggests that both the ash layer and the plug play a role in the reduced catalytic performance of an ash loaded DPF, and thus it is not necessarily advantageous to favor one mode of ash deposition over the other for the purpose of maintaining the catalytic activity of a DPF.

One of the key aspects of DPF performance is the ability of the filter to regenerate soot. This reaction was investigated using isothermal and controlled temperature ramp experiments. A major characteristic of any chemical reaction is the activation energy, which is a measure of the amount of energy required in order to initiate a particular reaction. The activation energy for active regeneration using O_2 was found to be 123 and 124 kJ/mol for the clean and the 42 g/L ash loaded samples respectively, well within the range of values reported in literature. The activation energy for passive regeneration using NO_2 was found to be 24 and 20 kJ/mol for the clean and the 42 g/L ash loaded samples respectively. These values are slightly below the range of expected values reported in literature, but are of the same order of magnitude. The consistency of activation energies between the clean and ash loaded samples indicate that ash accumulation does not alter the chemical reaction mechanism through which passive or active oxidation occurs.

It was found that the rate of reaction was lower for the 42 g/L ash loaded DPF than the clean sample. During an isothermal oxidation reaction, the peak CO_2 generation was reduced by 10% in the presence of ash. This is the critical finding of this work as it is clear evidence that the accumulation of ash has a negative impact on a DPF's ability to passively oxidize soot. Since the activation energy was not altered the reduction must be the result of a lower pre-exponential factor. This behavior could be caused by the physical masking of catalyst particles, the porous ash layer through which the NO_2 must back diffuse in order to oxidize the soot, the increased flow velocity resulting from the ash plug, or the effects of thermal aging.

6.2 Suggestions for Future Research

The experimental apparatuses and procedures described herein are highly adaptable. Several aspects of this study could be readily expanded in order to obtain a deeper understanding of the effects of ash accumulation on DPF catalytic activity.

The catalyst flow bench system could be improved by finalizing the flow bypass and water injection systems described in *Section 4.4.1*. Additionally, solenoid valves could be installed to enable pulsation of the flow and quartz tubes could be used to house the filters. All of these improvements would result in a higher degree of accuracy and operating conditions that are more representative of actual diesel exhaust.

In order to better understand the specific mechanisms through which the oxidation rate of soot is reduced, several targeted experiments could be conducted. The effect of the ash plug could be isolated by decreasing the volumetric flow through the filter such that the space velocity is computed using only the portion of the filter not occupied by the ash plug (as described in *Section 5.1.4.1*). The effect of reduced NO₂ generation resulting from ash could be explored by reducing the input NO_x concentration through a clean filter such that the magnitude of the NO₂ generated matches that of an ash loaded sample. The effect of thermal aging could be investigated by conducting all of the experiments described in this study with a DPF sample that has been put through the elevated temperature cycles experienced by the other aged samples but has not had any ash deposited on it.

Expanding the isothermal test matrix to include soot oxidation experiments at different temperatures could yield much more accurate Arrhenius Plots than those generated during temperature ramps. This would be a preferred method of obtaining values for the activation energies and pre-exponential factors for both active and passive regeneration inside the DPF.

Further experiments could be designed to determine whether ash impacts the reaction orders of soot oxidation via both O₂ and NO₂. Additionally, the microkinetic parameters that break down the reactions into their elementary steps could be investigated.

The test matrix could also be expanded to include more samples of laboratory and field aged DPFs, including those currently possessed by the Sloan Automotive Lab. These samples could

be used to investigate the impact of different lubricant/ash chemistries and regeneration strategies.

While a significant amount of research is still required in order to fully understand the effect of ash on the catalytic activity of DPFs and the impact it has on passive oxidation of soot, the results obtained in this study provide a useful starting point for further work. It was demonstrated that ash accumulation has a negative impact on catalyst performance, and that this results in a measurable reduction in the soot oxidation capabilities of a DPF. A deeper understanding of the mechanisms that cause this behavior could lead to improved design/operation strategies that could translate into improved DPF performance and engine fuel efficiency.

7 REFERENCES

- ¹ U.S. Energy Information Administration, "Energy Explained: Your Guide to Understanding Energy." [Online]. Available: <http://www.eia.gov/energyexplained/index.cfm>. [Accessed: 24-Mar-2014].
- ² Majewski, W. Addy, DieselNet Technology Guide, "Diesel Particulate Filters." [Online]. Available: <http://dieselnet.com/tech/dpf.php>. [Accessed: 24-Mar-2014].
- ³ Heywood, John B., Internal Combustion Engine Fundamentals, McGraw-Hill, Inc., New York, 1988.
- ⁴ Bullis, Kevin, MIT Technology Review, "A More Efficient Engine," [Online]. Available: <http://www.technologyreview.com/news/408352/a-more-efficient-engine/>. [Accessed: 25-Mar-2014].
- ⁵ Brokowski, M.E., Northwestern University, "CyclePad Design Library Entries," [Online]. Available: <http://www.qrg.northwestern.edu/thermo/design-library/>. [Accessed: 25-Mar-2014].
- ⁶ Jääskeläinen, H., Khair, M.K., DieselNet Technology Guide, "Diesel Engines," [Online]. Available: http://dieselnet.com/tech/diesel_engines.php. [Accessed: 25-Mar-2014].
- ⁷ U.S. Department of Energy: Office of Energy Efficiency & Renewable Energy, "Diesel Vehicles," [Online]. Available: http://www.fueleconomy.gov/feg/di_diesels.shtml. [Accessed: 25-Mar-2014].
- ⁸ European Automobile Manufacturers Association, "Statistics," [Online]. Available: <http://www.acea.be/statistics>. [Accessed: 25-Mar-2014].
- ⁹ Khair, Madgi K. et al., DieselNet Technology Guide, "Emission Formation in Diesel Engines," [Online]. Available: http://dieselnet.com/tech/diesel_emiform.php. [Accessed: 28-Mar-2014].
- ¹⁰ Kittelson, David B., "Engines and Nanoparticles: A Review," *Journal of Aerosol Science*, vol. 29, no. 5/6, pp. 575-588, 1998.
- ¹¹ Majewski, W. Addy, et al., DieselNet Technology Guide, "Engine Design for Low Emissions," [Online]. Available: http://dieselnet.com/tech/engine_design.php#limit. [Accessed: 02-Apr-2014].
- ¹² Ristovski, Zoran D., et al., 2012. "Respiratory health effects of diesel particulate matter." *Respirology (Carlton, Vic.)* 17, no. 2: pp. 201-212. *MEDLINE Complete*, EBSCO host (Accessed 02-Apr-2014).
- ¹³ Weinberger, Barry, et al., "The Toxicology of Inhaled Nitric Oxide," *Toxicology Science* (2001) 59 (1): 5-16 doi:10.1093/toxsci/59.1.5
- ¹⁴ United States Environmental Protection Agency, "Six Common Pollutants," [Online]. Available: <http://www.epa.gov/airquality/urbanair/>. [Accessed: 03-Apr-2014].
- ¹⁵ "Meeting EPA 2010." *FactsAboutSCR.com*. North American SCR Stakeholders Group, [Online]. Available: <http://www.factsaboutscr.com/environment/epa2010.aspx>. [Accessed: 03-Apr-2014].
- ¹⁶ EPA, 2014. "Control of Air Pollution from Motor Vehicles: Tier 3 Motor Vehicle Emission and Fuel Standards", US Environmental Protection Agency, Final Rule, EPA-HQ-OAR-2011-0135, [Online]. Available: <http://www.epa.gov/otaq/documents/tier3/tier-3-fr-preamble-regs-3-3-14.pdf>. [Accessed: 03-Apr-2014].
- ¹⁷ Majewski, W. Addy, DieselNet Technology Guide, "Diesel Particulate Filters," [Online]. Available: <http://dieselnet.com/tech/dpf.php>. [Accessed 07-Apr-2014]

-
- ¹⁸ Konstandopoulos, A. G., et al., "Fundamental Studies of Diesel Particulate Filters: Transient Loading, Regeneration and Aging," SAE 2000-01-1016, 2000.
- ¹⁹ van Setten, Barry A., et al., "Science and Technology of Catalytic Diesel particulate Filters," *Catalysis Reviews: Science and Engineering*, 43:4, pp. 489-564, 2001.
- ²⁰ Frobert, A., et al., "Generating Thermal Conditions to Regenerate a DPF: Impact of the Reductant on the Performances of Diesel Oxidation Catalysts," SAE International 2009-01-1085, 2009.
- ²¹ Goldenberg, E., "Depollution des gaz d'echappement des moteurs Diesel au moyen de pots catalytiques", *Revue Institut Francais du Petrole*, vol. 38, pp.793-805, 1983.
- ²² Sappok, A., and Wong, V., "Detailed Chemical and Physical Characterization of Ash Species in Diesel Exhaust Entering Aftertreatment Systems," SAE 2007-01-0318, 2007.
- ²³ Sappok, A., Wong, V., "Ash Effects on Diesel Particulate Filter Pressure Drop Sensitivity to Soot and Implications for Regeneration Frequency and DPF Control," SAE 2010-01-0811, 2010.
- ²⁴ Aravelli, K., Heibel, A., "Improved Lifetime Pressure Drop Management for Robust Cordierite (RC) Filters with Asymmetric Cell Technology (ACT)," SAE 2007-01-0920, 2007.
- ²⁵ McGeehan, J., et al., "API CJ-4: Diesel Oil Category for Both Legacy Engines and Low Emission Engines Using Diesel Particulate Filters", SAE Technical Paper 2006-01-3439, 2006.
- ²⁶ Ishizawa, T., et al., "Investigation into Ash Loading and its Relationship to DPF Regeneration Method," SAE International 2009-01-2882, 2009.
- ²⁷ Bodek, K. M., Wong, V., "The Effects of Sulfated Ash, Phosphorus and Sulfur on Diesel Aftertreatment Systems – A Review," SAE International 2007-01-1922, 2007.
- ²⁸ Lambert, Christine K., et al., "Post Mortem of an Aged Tier 2 Light-Duty Diesel Truck Aftertreatment System," SAE International 2009-01-2711, 2009.
- ²⁹ Sappok, A., DieselNet Technology Guide, "Ash Accumulation in Diesel Particulate Filters," [Online]. Available: http://dieselnet.com/tech/dpf_ash.php#sources. [Accessed 10-Apr-2014].
- ³⁰ Kamp, C. J., et al., "Direct Measurements of Soot/Ash Affinity in the Diesel Particulate Filter by Atomic Force Microscopy and Implications for Ash Accumulation and DPF Degradation," SAE International 2014-01-1486, 2014.
- ³¹ Sappok, A., et al., "Investigation of Ash Formation, Accumulation, and Distribution in Diesel Particulate Filters Using Lubricant Additive Tracers," *Proceedings of the ASME 2011 Internal Combustion Engine Division Fall Technical Conference*, ICEF2011-60072, 2011.
- ³² Sappok, A., Wang, Y., Wang, R., Kamp, C. et al., "Theoretical and Experimental Analysis of Ash Accumulation and Mobility in Ceramic Exhaust Particulate Filters and Potential for Improved Ash Management," SAE International 2014-01-1517, 2014.
- ³³ Jääskeläinen, H., DieselNet Technology Guide, "Engine Exhaust Back Pressure," [Online]. Available: http://dieselnet.com/tech/diesel_exh_pres.php. [Accessed: 10-Apr-2014].
- ³⁴ Sappok, Alexander, Wong, Victor W., "Lubricant-Derived Ash Properties and their effects on Diesel Particulate Filter Pressure Drop Performance," *Proceedings of the ASME 2009 Internal Combustion Engine Division Fall Technical Conference*, ICEF2009-14080, 2009.

-
- ³⁵ Levenspiel, Octave, Chemical Reaction Engineering, 2nd Edition, John Wiley & Sons, Inc., New York, 1972.
- ³⁶ AP Chemistry Lab, "Review Topic 2," [Online]. Available: http://soul-linked.blogspot.com/2013_04_01_archive.html. [Updated: 18-Apr-2013, Accessed: 18-Apr-2014].
- ³⁷ DieselNet Technology Guide, "Catalyst Fundamentals," [Online]. Available: http://dieselnet.com/tech/cat_fund.php. [Accessed: 21-Apr-2014].
- ³⁸ DieselNet Technology Guide, "Catalyzed Diesel Filters," [Online]. Available: http://dieselnet.com/tech/dpf_cat.php. [Accessed 21-Apr-2014].
- ³⁹ Haralampous, O. A., et al., "Reaction and Diffusion Phenomena in Catalyzed Diesel Particulate Filters," SAE Technical Paper 2004-01-0696, 2004.
- ⁴⁰ Lee, J. H., et al., "Experimental Investigation of Soot Oxidation Characteristic with NO₂ and O₂ using a Flow Reactor Simulating DPF," SAE Technical Paper Series 2007-01-1270, 2007.
- ⁴¹ Wang-Hansen, C., "Kinetic Analysis of Automotive Soot Oxidation: Development and Applications of Experimental Evaluation Methods," Chalmers University of Technology, 2012.
- ⁴² Jelles, S., J., "Diesel Particulate Control: Application of Activated Particulate Trap in Combination with Fuel Additives at an Ultra Low Dose Rate," SAE Technical Paper 1999-01-0113, 1999.
- ⁴³ Kamp, C., J., "Multiscale Methods for the Fundamental Understanding of Diesel Soot Mitigation," Chalmers University of Technology, 2011.
- ⁴⁴ Kamp, C., J., et al., "Soot and Ash Deposition Characteristics at the Catalyst-Substrate Interface and Intra-Layer Interactions in Aged Diesel Particulate Filters Illustrated using Focused Ion Beam (FIB) Milling," SAE International 2012-01-0836, 2012.
- ⁴⁵ Sappok, A. G., "The Nature of Lubricant-Derived Ash-Related Emissions and Their Impact of Diesel Aftertreatment System Performance," Massachusetts Institute of Technology, 2009.
- ⁴⁶ Sappok, A. G., et al., "A Novel Accelerated Aging System to Study Lubricant Additive Effects on Diesel Aftertreatment System Degradation," SAE International 2008-01-1549, 2008.
- ⁴⁷ MKS Instruments, Inc., "MultiGas™ 2030 FTIR Continuous Gas Analyzer," [Online]. Available: <http://www.mksinst.com/product/product.aspx?ProductID=180>. [Accessed 06-May-2014].
- ⁴⁸ DieselNet Technology Guide, "Gaseous Emissions," [Online]. Available: http://dieselnet.com/tech/emi_gas.php#nox. [Accessed 06-May-2014].



(This page intentionally left blank)

APPENDIX

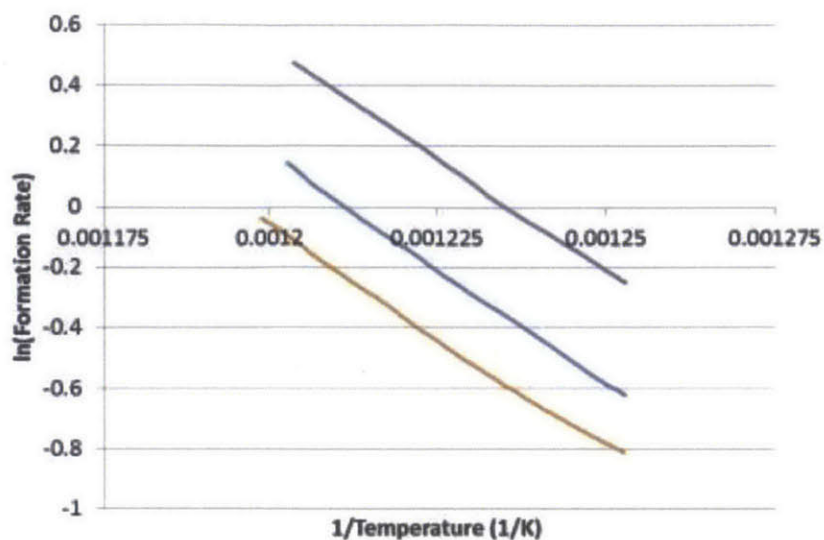


Figure A.1 Arrhenius Plot of Soot Oxidation: Active O₂ Mechanism for 42 g/L Ash Loaded DPF Repeated

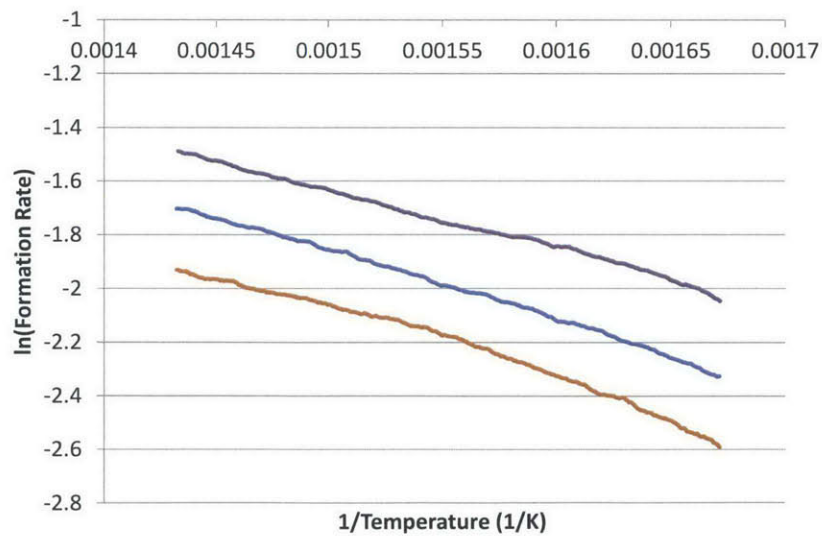


Figure A.2 Arrhenius Plot of Soot Oxidation: Passive NO₂ Mechanism for 42 g/L Ash Loaded DPF Repeated